

**BAYESIAN RESERVOIR CHARACTERIZATION BASED ON
SIMULTANEOUS SEISMIC INVERSION
EXAMPLE: OFFSHORE EAST JAVA CARBONATE**

THESIS

FAHDI MAULA
0706171900



UNIVERSITAS INDONESIA
FACULTY OF MATHEMATICS AND NATURAL SCIENCES
PHYSICS GRADUATE PROGRAM
JAKARTA
DECEMBER 2009

**BAYESIAN RESERVOIR CHARACTERIZATION BASED ON
SIMULTANEOUS SEISMIC INVERSION
EXAMPLE: OFFSHORE EAST JAVA CARBONATE**

THESIS

Submitted in Partial Fulfillment of the Requirements for the Degree of Master of
Science in Reservoir Geophysics

FAHDI MAULA

0706171900

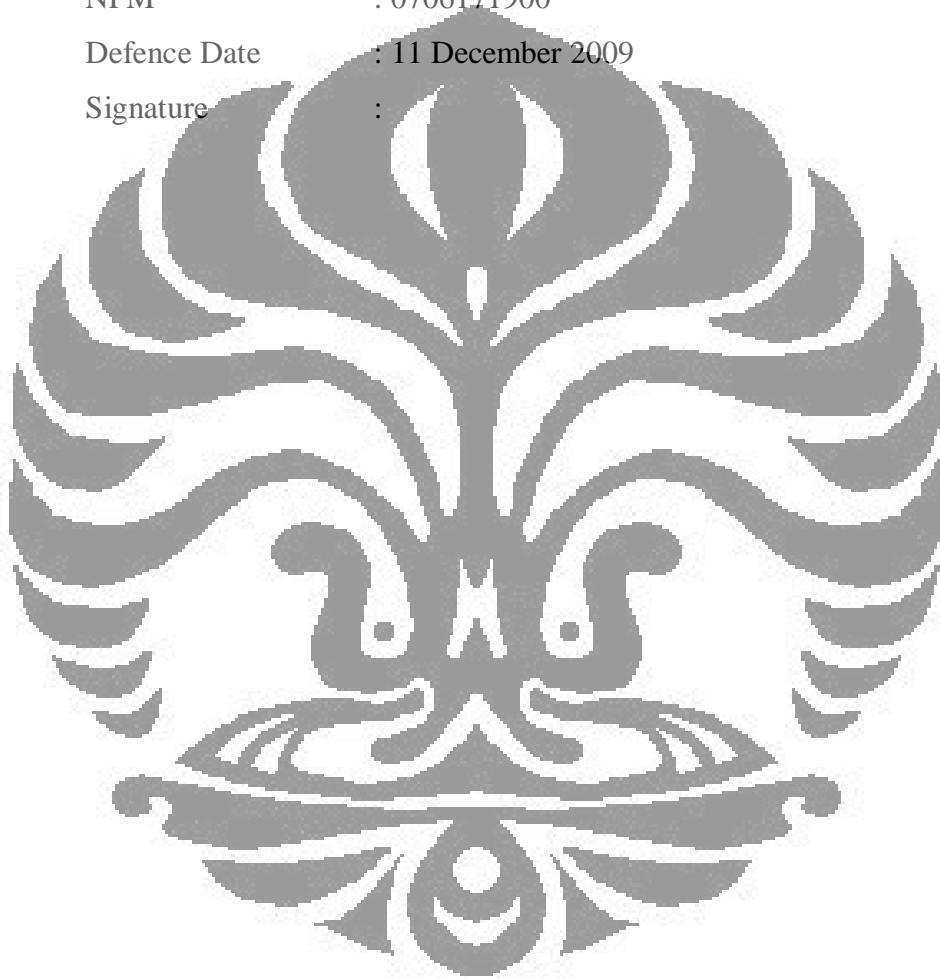


UNIVERSITAS INDONESIA
FACULTY OF MATHEMATICS AND NATURAL SCIENCES
PHYSICS GRADUATE PROGRAM
RESERVOIR GEOPHYSICS PROGRAM
JAKARTA
DECEMBER, 2009

Originality

I hereby notify that this thesis is my original work, and all of the sources that has been cited or referred has been explained or stated clearly.

Name : Fahdi Maula
NPM : 0706171900
Defence Date : 11 December 2009
Signature :



Approval Page

Thesis submitted by,

Author Name : Fahdi Maula

NPM : 0706171900

Program : Reservoir Geophysics Graduate Program,
Physics Graduate Program,

Faculty of Mathematics and Natural Sciences

Title : Bayesian Reservoir Characterization Based on
Simultaneous Seismic Inversion Example: Offshore
East Java Carbonate

Has been successfully defended in front of committee members and accepted as partial fulfillment of the requirements for the Degree of Master of Science in Reservoir Geophysics at Reservoir Geophysics Graduate Program, Faculty of Mathematics and Natural Sciences, Universitas Indonesia

Advisor : Dr. Abdul Haris ()

Examiner : Prof. Dr. Suprajitno Munadi ()

Examiner : Dr. Adriansyah ()

Examiner : Dr. Charlie Wu ()

Approved in Jakarta

Date : 11 Desember 2009

Acknowledgment

I would like to acknowledge and give the utmost respect for the following people and organizations, without their contribution this thesis will never be completed. For this, I humbly thank each one of them; although many more contributed and I am deeply regret not to put them in this list for practical reasons.

Dr Abdul Haris, as supervisor for this thesis, I would like to thank his willingness to share his knowledge and experience in completing this thesis, despite his workload in teaching and advising other students will always be appreciated.

Prof. Dr. Suprajitno Munadi, I would like give my utmost respect for his dedication in teaching and development of geophysical research in Indonesia. Professor Munadi not only contributed as being one of my thesis examiners, but also giving guidance since the very beginning of writing this thesis proposal.

Dr. Adriansyah, who had been the member of my thesis committee, is acknowledged for his willingness to share his valuable time in reviewing this work. I would also thank him for his dedication in teaching and words of wisdom on becoming good scientist, since I first met him in Diklatsar HMGE ITB around 2001-2002.

Dr. Charlie Wu, who had been the member of my thesis committee, is acknowledged for his willingness to share his valuable time in reviewing this work. I personally would like to thank Dr. Charlie Wu for introducing me to the beautiful theory of Markov Chain, and his lecture on Geostatistic is very inspiring.

I thank Sri Lestari, M.Si and Agung Roniwibowo, M.Si, from Pearl Energy Ltd., to help me providing the opportunity to work with their data. Without their support, I will never move from the start line. I also personally thank Didik Ardianto, M.Si., for giving the opportunity to work side by side with him in using the data given by Pearl Energy.

I thank Geophysics DCS-RSS Schlumberger Jakarta, especially to Bruce Shapiro, Wahyu Prasetya, and Pierre Bihan for their understanding and their support to finish this thesis. All the geoscientists and engineers in DCS Jakarta are acknowledged for their support in completing my graduate study.

I thank my family, in Jakarta for supporting me in doing graduate study. With this thesis, I hope I encourage my brother, Fazlul Rahman, to always keep his spirit up in finishing his graduate study in Islamic University of Indonesia, Jakarta.

I also would like to express my sincere thanks to Befriko Murdianto, M.Si., he has been very supportive in giving guidance to me about seismic processing, inversion, and especially about Bayesian theorem. This thesis is very much inspired by his thesis about Bayesian theorem in 2007. I also would to pay respect to my senior in Geophysics and Meteorology ITB, Yasser Taufiq, S.Si, for always encourage to never give up and keep exploring the beauty of geophysics.

Finally, I would like to express my respect and thank to Genia Atma Nagara, M.Sc., there is no words that can describe how her support is the reason why I can type each and every words in this thesis.

Fahdi Maula

Abstract

Bayesian fluid classification and Bayesian porosity-saturation estimation has been done using simultaneous seismic inversion result as the input in Kujung carbonate from East Java Basin, Indonesia. Many literatures described the limitation of carbonate characterization based on AVO anomaly. This study carried out to present the classification and estimation result with level of confidence based on Bayesian theorem.

We have done two phases of characterization, qualitative and quantitative. In qualitative characterization, two classes of fluid were defined, these are gas and wet. Before any new information, it is assumed that the prior probability density function (PDF) of these two classes is the same, 50:50. Initial distribution of each wet and gas filled carbonate were then estimated from well log data, these are the likelihood function. Acoustic impedance, V_p/V_s ratio, and density were then derived from 3D multi stacks seismic data using simultaneous AVO inversion. These attributes are the new information required to update our prior distribution to have final posterior PDF using Bayesian theorem that represent fluid classification for each traces. In the other process for quantitative characterization, the porosity and saturation distribution were defined using basic velocity to porosity & saturation relationship (rock physics analysis). The prior PDF is defined based on analyzed well data, and stochastic simulation was done to generate likelihood function to form joint PDF between porosity and saturation, before finally applied to estimate porosity and saturation cube using Bayesian Scheme.

The final product of the proposed workflow is 3D fluid cube of reservoir with associated probabilities and uncertainties which consist of probability of wet carbonate and gas carbonate, also quantitative estimation of porosity and saturation. The result shows that potential pay zone for this particular carbonate was lying on the flank of the buildup carbonate.

Abstrak

Klasifikasi fluida serta estimasi porositas berdasarkan teorema Bayes telah dilakukan dengan menggunakan hasil inversi seismik simultan sebagai inputnya pada karbonat formasi Kujung di cekungan Jawa Timur, Indonesia. Banyak literatur yang menjelaskan ambiguitas dari karakterisasi batuan karbonat berdasarkan anomali AVO. Studi ini dilakukan untuk menghasilkan klasifikasi dan estimasi yang memiliki tingkat kepastian berdasarkan teorema Bayes.

Kami melakukan dua fasa karakterisasi, kualitatif dan kuantitatif. Dalam karakterisasi secara kualitatif, 2 kelas/tipe fluida didefinisikan, yaitu gas dan wet. Sebelum ada informasi baru, diasumsikan probabilitas prior dua kelas ini adalah sama, 50:50. Distribusi probabilitas awal dari dua kelas ini kemudian ditentukan melalui data sumur, distribusi ini akan menjadi likelihood function. Impedansi akustik, rasio V_p/V_s , dan densitas kemudian diturunkan dari inversi seismik simultan. Atribut ini adalah informasi baru yang akan digunakan untuk mengupdate probabilitas prior tadi menjadi probabilitas posterior dengan menggunakan teorema Bayes, probabilitas posterior ini merepresentasikan klasifikasi fluida pada setiap tras seismik. Dalam proses lainnya untuk karakterisasi secara kuantitatif, distribusi porositas dan saturasi didefinisikan menggunakan hubungan dasar kecepatan terhadap porositas dan saturation. Probabilitas prior didefinisikan berdasarkan data sumur, kemudian simulasi stokastik dilakukan untuk menghasilkan likelihood function yang membentuk probabilitas bersama antara porositas dan saturasi, sebelum akhirnya diaplikasikan untuk estimasi porositas dan saturasi berdasarkan skema Bayes.

Hasil akhir dari langkah kerja ini adalah data 3D dari tipe fluida yang berasosiasi dengan probabilitas dan ketidakpastian untuk tiap posisi. Data 3 dimensi ini terdiri atas probabilitas wet, probabilitas gas, dan juga estimasi kuantitatif dari porositas dan saturasinya. Hasil langkah kerja pada area studi kami menunjukkan potensi pay zone berada pada flank dari buildup carbonate tersebut

Table of Contents

Originality	i
Approval Page	ii
Acknowledgment	iii
Abstract	v
<i>Abstrak</i>	vi
Table of Contents	vii
Table of Figures	ix
CHAPTER 1 INTRODUCTION	1
1.1. Thesis Objective	2
1.2. Area of Study	2
1.3. Data Used	5
1.4. Problem Limitation	5
1.5. Thesis Structure	6
1.6. Hardware and Software	6
CHAPTER 2 THEORY AND METHODOLOGY	7
2.1 Methodology	7
2.2 Biot-Gassmann Theory	10
2.2.1. Velocity-Porosity & Saturation Analysis	11
2.3 Simultaneous Seismic Inversion	13
2.2.1. Aki-Richards Equations	13
2.4 Bayesian Theorem	16
CHAPTER 3 PETROPHYSICS AND BASIC ROCK PHYSIC ANALYSIS	20
3.1. Petrophysical Analysis	20
3.2. Fluid Replacement Modeling	21
3.3. Synthetic AVO Modeling	24

3.4. Velocity-Porosity Relationship Analysis.....	25
CHAPTER 4 SIMULTANEOUS SEISMIC INVERSION	26
4.1. Angle Stack Alignment	26
4.2. Log Calibration and Wavelet Extraction	28
4.3. Low Frequency Modeling.....	30
4.4. Inversion	32
CHAPTER 5 BAYESIAN RESERVOIR CHARACTERIZATION.....	38
5.1. Fluid Classification	38
5.2. Joint-Porosity Saturation Modeling	45
CHAPTER 6 DISCUSSION AND RECOMMENDATION	50
Rock Physics Model for Carbonate	50
Porosity-Saturation Estimation.....	50
REFERENCES.....	52

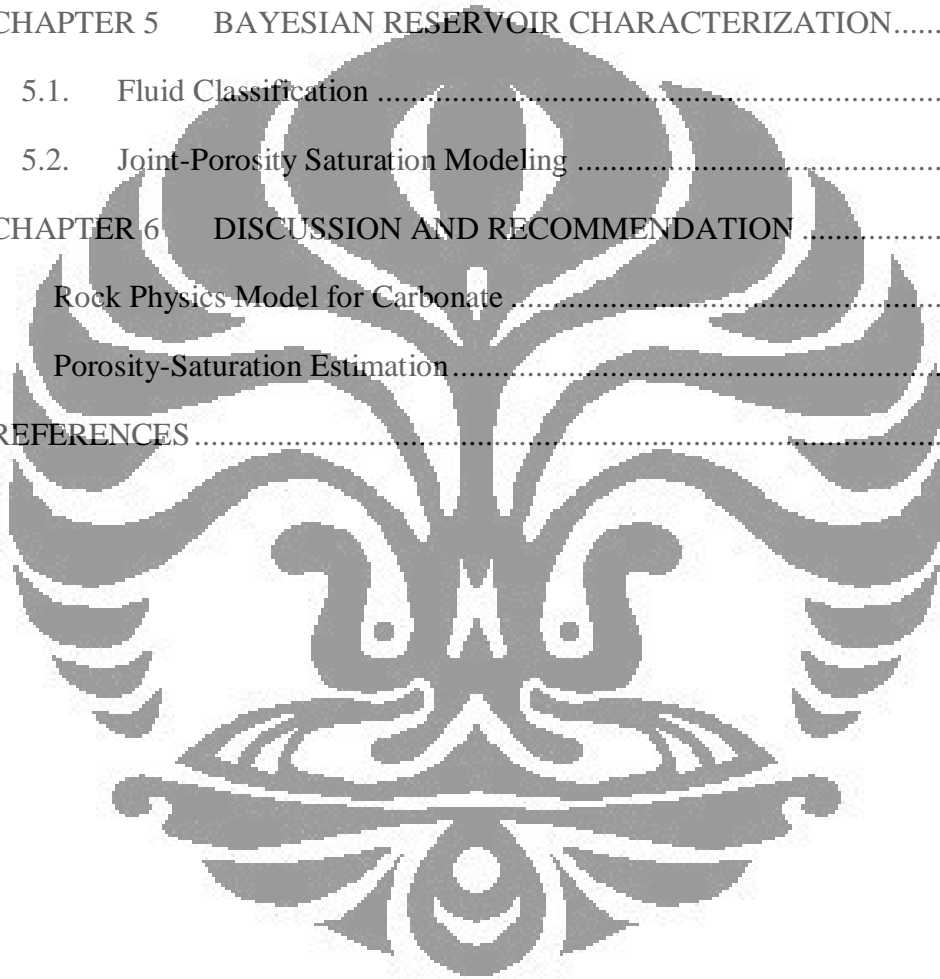


Table of Figures

Figure 1.1. Location of Area of Study (Peal Energy Internal Report)	2
Figure 1.2. East Java Basin Stratigraphy (Peal Energy Internal Report).....	3
Figure 1.3. Kujung-I time structure	4
Figure 1.4. Flat Spot Anomaly	5
Figure 2.1. Diagram for Qualitative Characterization	8
Figure 2.2. Diagram of Quantitative Reservoir Characterization	9
Figure 2.3. Hashin-Shtrikman Bounds	12
Figure 2.4. Comparison between separate inversion and Simultaneous inversion (Maver, 2004)	14
Figure 3.1. Petrophysical analysis of AGR-1 (Pearl Energy Internal Report, 2009), zone of interest marked with yellow circle.....	21
Figure 3.2. Crossplot AI vs Vp/Vs vs Sw over Kujung Interval.....	22
Figure 3.3. Elastic Log after Substituted to 100% water (red is in situ measured log, blue after substituted to 100% water).....	23
Figure 3.4. Synthetic Gather Modeling	24
Figure 3.5. Porosity-Elastic Moduli Relationship	25
Figure 4.1. Alignment in one In-line on near to mid alignment, without filtering (top-left) with horizontal filtering (top-right). Lateral time-shift map (bottom)	27
Figure 4.2. Synthetic seismogram inserted into each angle stack (near-left, mid- middle, far-right) shows good correlation on zone of interest.....	29
Figure 4.3. Comparison of measured seismic amplitude with modeled amplitude using extracted wavelet for near (left) , mid (middle), and far (right)	29
Figure 4.4. Summary of extracted wavelet	30
Figure 4.5. Frequency content of near (left), mid (center), far (right) stack.....	31
Figure 4.6. Low Frequency Model for AI (left), Vp/Vs Ratio (middle), and density (right).....	31
Figure 4.7. AI Inversion result and it's comparison with measured AI	34

Figure 4.8. Vp/Vs ratio inversion result and its comparison with measured Vp/Vs	35
Figure 4.9. Density inversion result compared to measured density	36
Figure 4.10. Comparison of time slice fullstack amplitude, AI cube, and Vp/Vs cube	37
Figure 5.1. Prior Distribution	39
Figure 5.2. Comparison of fluid classification (left) with fullstack amplitude (right). Black curve in the middle is Sw.....	40
Figure 5.3. Comparison of seismic amplitude (a) with classification result (b), and the input for classification Vp/Vs (d) and AI (d) Noted that flat spot defined as boundary between gas and water, taken from offset XLine from AGR-1 well (log curve is Sw). Red arrow shows flatspot.....	43
Figure 5.4. Time Structure with classification map as color scale from 25 ms below Kujung-I, blue is gas, yellow is wet, and white is undetermined.....	44
Figure 5.5. Time Structure map with gas probability as color scale from 25 ms below Kujung-I.....	44
Figure 5.6. (a) Porosity-bulk modulus crossplot and 2 nd order polynom fitting, (b) Water saturation vs Porosity crossplot.....	45
Figure 5.7. Simulation result (left) Joint porosity-saturation PDF (right).....	46
Figure 5.8. Comparison of seismic amplitude (top left), gas probability (top right), porosity (mid), and water saturation (bottom). AGR-1 well marked with inserted curve in the plot.....	48
Figure 5.9. Time Structure map with porosity as color scale from 25 ms below Kujung-I	49
Figure 5.10. Time structure map with water saturation as color scale from 25 ms below Kujung-I.....	49

CHAPTER 1

INTRODUCTION

A review on literature suggests that relationships among reservoir parameter such as V_p , V_s , and density in carbonates reservoir are scattered. Adriansyah (2001) noted that the main exploration issue for carbonate reservoirs in northwest Java basin, Indonesia was determining the porosity distribution within the reefs. By analyzing Parigi formation, Adriansyah (2001) reported that porosity calculation using various techniques such as time average were widely scattered. In conclusion, porosity still could not be determined solely from V_p , V_s , and density even if the lithology was fairly well constrained. Chacko (1989) reported success story for application of AVO to map porosity in Baturaja limestone in South Sumatra. He also reported V_p/V_s which normally worked for detecting effect of gas-filled sand did not work for gas-filled limestones. He concluded the V_p/V_s ratio for South Sumatra limestone was controlled by the mineralogy rather than by porosity or pore fluid. Thus, we cannot rely on standard impedance to porosity transformation. Detailed mineralogy and fluid effect modeling need to be conducted. In other cases, Carter et al. (2005) published their analysis on Kujung-I carbonate in East Java Basin. One of their analyses was about non linear relationship between acoustic impedance and porosity for Kujung-I reservoir. They concluded, that the low acoustic impedance and low amplitude in Kujung-I were generally positive indicators of porosity and sometimes gas.

Having described the issues of carbonate reservoirs exploration limited to Indonesian area, it may conclude that new understanding of dealing with elastic properties and their relation to reservoir parameters is needed. An understanding about how to accurately map the potential carbonate pay zone using seismic data is highly required. Due to some complexities in carbonate body, it is also required to qualitatively determine the reservoir potential based on comprehensive knowledge that we gathered in the area.

This thesis described the workflow for fluid prediction based on 3D seismic data on a carbonate reservoir in Indonesia. To obtain reliable reservoir characterization using 3D seismic data, three main steps were taken: conducting accurate seismic inversion to obtain relevant reservoir parameters, rock physics transformation to relate reservoir parameters to the seismic parameters, and mapping the parameters in 3D space (Bachrach et al., 2004). The final product of the proposed workflow is 3D map of reservoir properties with associated probabilities and uncertainties.

1.1. Thesis Objective

The goal of this thesis is to qualitatively and quantitatively identify carbonate reservoir hydrocarbon potential, by classifying their fluid content based on measured well log data and estimation of porosity and saturation using rock physics relationship. This classification and estimation will be mapped into 3D space guided by elastic attribute derived from simultaneous seismic inversion using Bayesian theorem.

1.2. Area of Study

In this thesis, the analysis was conducted in carbonate reservoir in AGR Block, in East Java Basin. This block is operated by Pearl Energy, Ltd. Approximately located 80 Km from Tuban city, and 160 Km from Surabaya.



Figure 1.1. Location of Area of Study (Peal Energy Internal Report)

The exploration objective was to evaluate gas potential within Kujung carbonate build-up and Tuban Sandstones up-dip from the Kepodang Gas Field, and also oil potential in basal clastic which pinched out against basement. Specific for this

study I will focus in gas analysis of Kujung Carbonate build-up. Figure below showing regional stratigraphy of the East Java Basin.

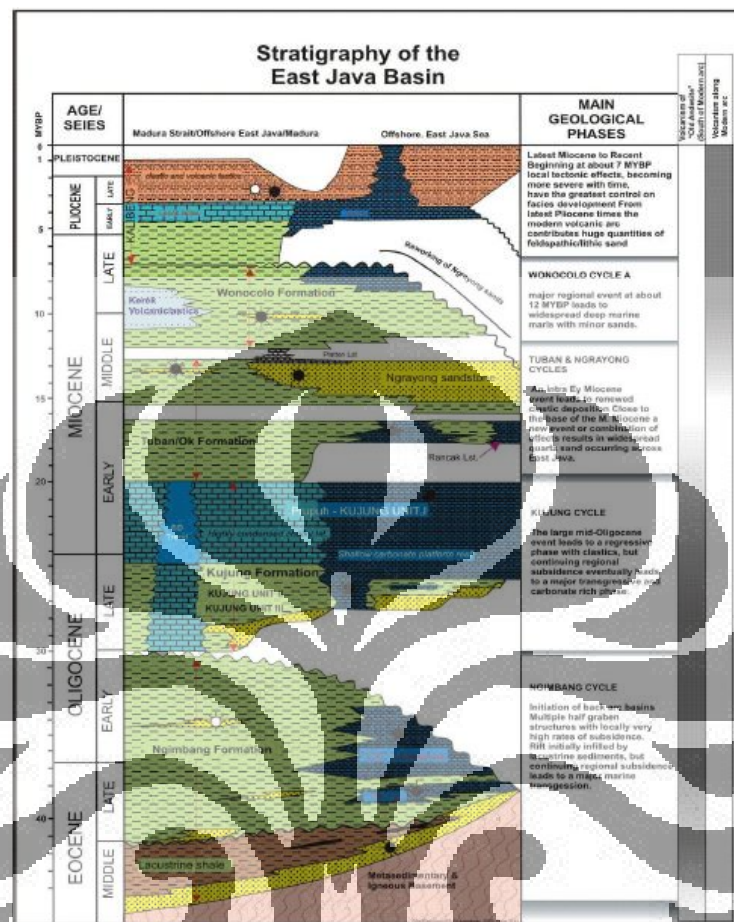


Figure 1.2. East Java Basin Stratigraphy (Pea Energy Internal Report)

Kujung carbonate in this study was divided into two zones, Kujung-I and Kujung-II. The reservoir might have been sourced from both the east and the west. From the analyses of previous wells, it was recovered that Kujung unit I and II contained gas with high CO_2 . This CO_2 was analyzed to be generated from Muriah and Lasem volcanoes which intruded the Kujung shelf at approximately 1.0 MYBP. In addition, the reservoir in this might be sourced from the Bawean Trough to the East. Based upon maturity mapping, the Ngimbang Formation source rocks are currently within the oil window. During tectonic quiescence prior to the regional inversion event the preferred direction for migration was along the sediment-basement interface, updip to the west onto the paleo high. This potential

Kujung reservoir was regionally sealed with the Tuban and Wonocolo (Pearl Energy Internal Report, 2009).

In the newly acquired 3D seismic data, the time interpretation of Kujung-I event shows that Kujung-I is recognized as carbonate build up. Figure below showing time structure map of area of study, there is a high structure zone (marked in purple circle) in North East of survey area which might be the perfect trap in the petroleum system.

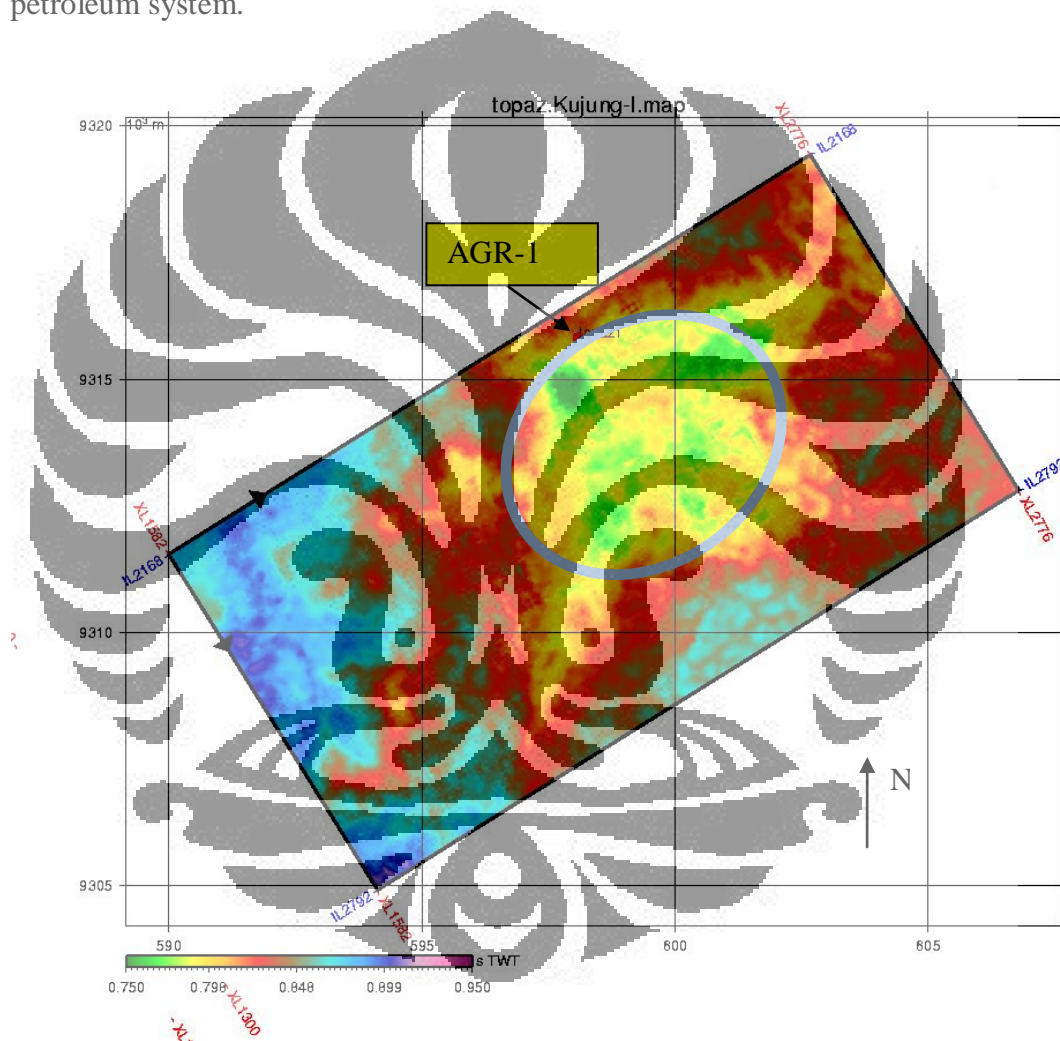


Figure 1.3. Kujung-I time structure

The seismic inversion was intended to see the property within Kujung carbonate. Valuable information which can be seen from seismic data was the presence of flat spot anomaly. This anomaly was suspected to be gas-water-contact in Kujung-

I reservoir. It is expected that seismic inversion can turn this anomaly into more meaningful reservoir properties.

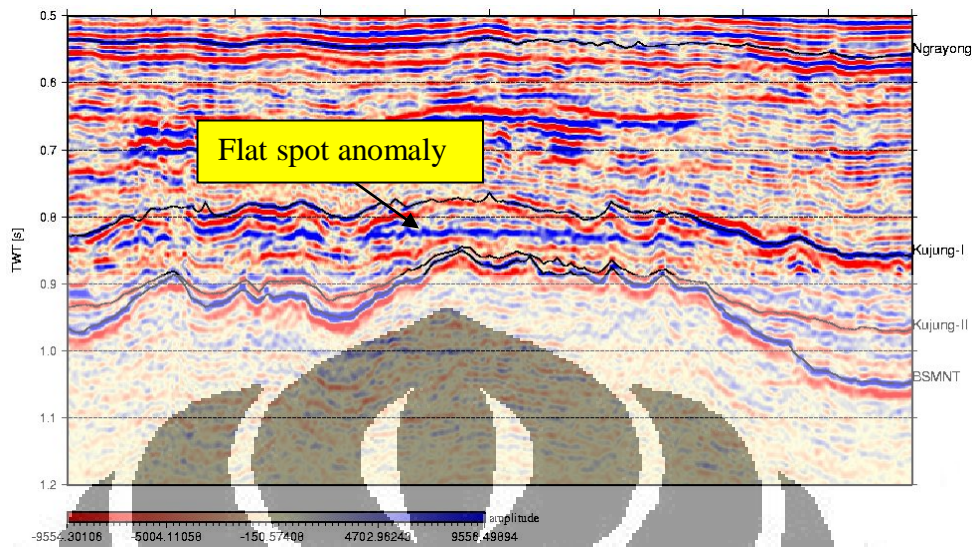


Figure 1.4. Flat Spot Anomaly

1.3. Data Used

To support this study, following data was used in the area of study,

- 3D Angle Stack Seismic:
 - Near Angle Stack : 0-13 degree
 - Mid Angle Stack : 13-26 degree
 - Far Angle Stack : 26-39 degree
- 1 well data was available, AGR-1, log data are gamma ray, caliper, deep resistivity, density, neutron porosity, compressional sonic log, shear sonic log, checkshot data, and also petrophysical log analysis (VClay, Water Saturation, and Porosity)

1.4. Problem Limitation

One major issue with fluid content analysis within carbonate reservoir is the applicability of Biot-Gassmann theory. In this thesis, Biot-Gassmann theory was assumed to be applicable for this case.

1.5. Thesis Structure

This thesis consisted of six chapters. The first chapter (Introduction) states the general overview of the thesis and the objectives of this study. In chapter 2, theory and methodology for Bayesian reservoir characterization are discussed. These theories include about Biot-Gassmann Theory, Velocity-Porosity and Saturation relationship, Simultaneous Seismic Inversion, and Bayesian Theorem.

Chapter 3 contains well log analysis and synthetic. Objectives of chapter three are the lithology and fluid class definition. The synthetic modeling which was used in chapter three is Biot-Gassmann fluid substitution and AVO Synthetic Modeling. Within this chapter basic rock physics analyses was conducted to determine the relation between porosity, saturation and elastic moduli.

Explanation and analysis about simultaneous seismic inversion method that were used in the study are included in chapter 4. It consists of preprocessing, log calibration and wavelet extraction, low frequency modeling, and inversion. At the beginning of chapter 5, analyses of the lithology and fluid class mapping from well log into 3D space are explained.

In chapter 6, general discussion is drawn from all previous 5 chapters. Conclusion and suggestion for further research about this topic are also mentioned.

1.6. Hardware and Software

The thesis work was done with the help of Pearl Energy Ltd. and Schlumberger DCS Jakarta, Indonesia. Data for analysis was given by the courtesy of Pearl Energy Ltd. Software for working in this thesis was supported by the help of Schlumberger Data and Consulting Services, Jakarta, Indonesia.

Seismic inversion and lithology cube definition was done using *Schlumberger ISIS* and *Schlumberger MMRD* software in Schlumberger DCS Jakarta office. The *Hampson-Russell* software used for log analysis was provided by University of Indonesia. Report assembly was done using *Microsoft Word*.

CHAPTER 2

THEORY AND METHODOLOGY

Before analyzing and discussing further about application of Bayesian Theorem in reservoir characterization, ground theory (rock physics theory) of relating seismic attributes (such as V_p , V_s , and density) to reservoir properties (such as porosity and saturation) needs to be discussed. General Bayesian theorem which was used to classify fluid and to estimate porosity/saturation was also discussed in this chapter.

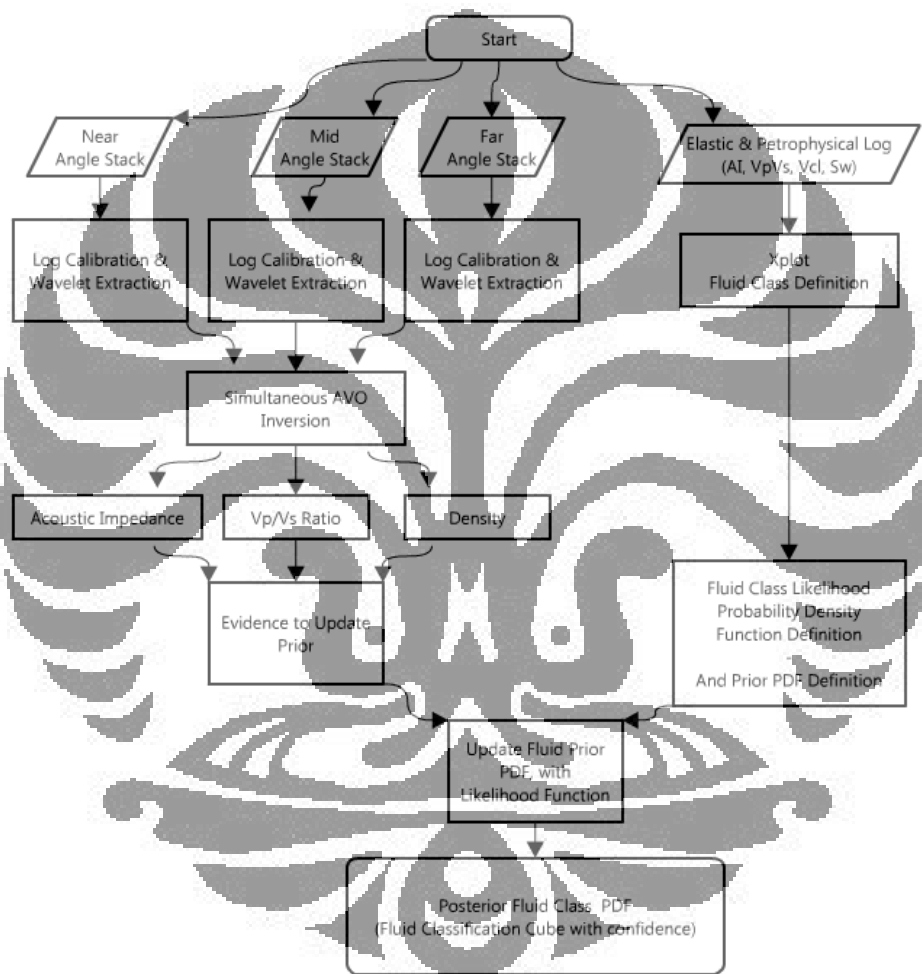
2.1 Methodology

The methodology to characterize the reservoir will be divided into two main parts. First is the qualitative characterization, which has the objective to classify gas zone and wet zone with associated level of confidence. The second main part is the quantitative characterization, with the objective to estimate porosity and saturation from seismic inversion result.

Diagram below (figure 2.1) summarizes the qualitative characterization from seismic inversion result. The flow starts by doing petrophysical analysis/formation evaluation. Petrophysical analysis will define the pay zone characteristic. By doing cross plotting of elastic attribute, two main fluid classes will be defined based on V_{cl} , $PHIT$, and elastic appearance. These classes are gas class and wet class. For each class, probability density function will be built. This probability density function will be the likelihood probability density function as the input for Bayesian classification.

Aligned with the petrophysical analysis, well to seismic tie was performed to tie log event with seismic event. This log calibration was done to all angle stacks. The result of log calibration is wavelet which will be used in the inversion process. Each angle stack will have specific wavelet to be used in the inversion. Inversion process will need low frequency model as a start point of the model; this model was also built from interpolation of calibrated log to seismic data based on

interpreted horizon. All these preparations required to run simultaneous seismic inversion in order to extract 3D elastic cube for fluid classification mapping. Required product of the simultaneous inversion to be used in classification mapping will be based on how the prior model was built. In this study, the prior model was built based on probability density function of acoustic impedance and Vp/Vs ratio. Therefore, inversion is required to output acoustic impedance cube and Vp/Vs ratio cube.



Made with lovelycharts.com

Figure 2.1. Diagram for Qualitative Characterization

Diagram in figure 2.2 below summarized the workflow for quantitative reservoir. The flows start by building rock physics analysis using elastic attribute and petrophysical log. The objective is to have rock physics model and build prior probability density function based on measured well data. Stochastic simulation will be done to explore all ranges of porosities and saturation and to simulate the sediment elastic responses associated with the rock physics forward model described previously. Joint PDF of porosity and saturation after stochastic simulation will be built representing the likelihood function.

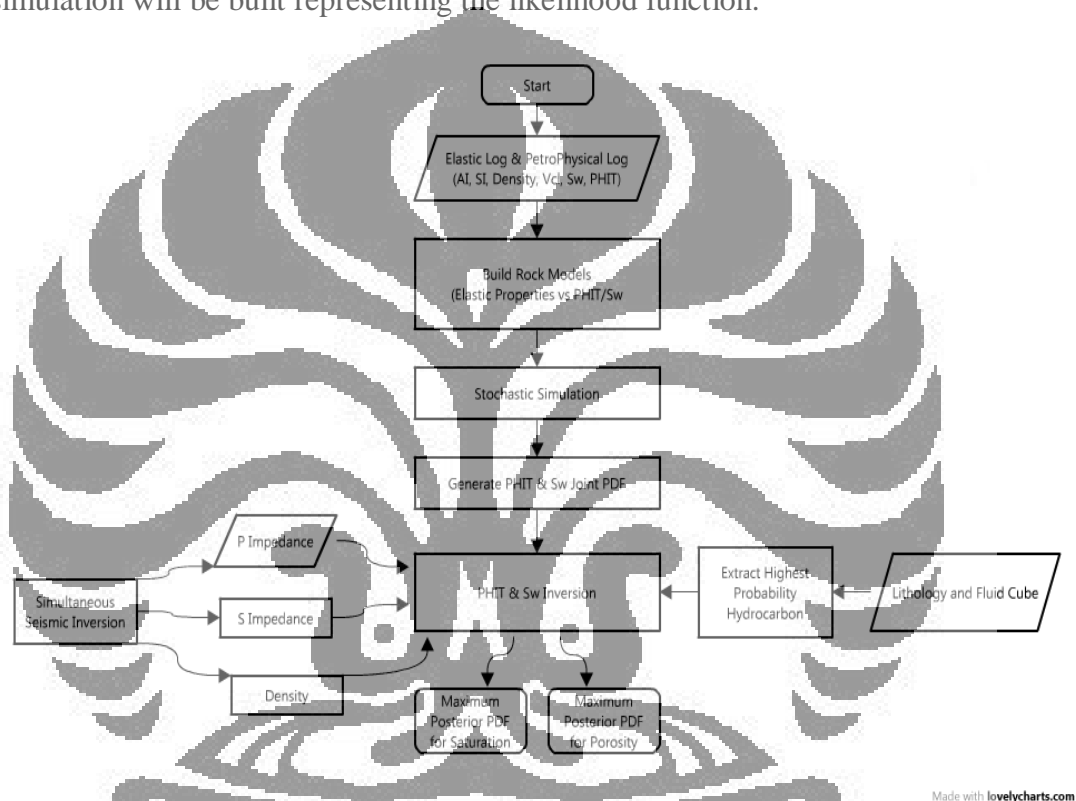


Figure 2.2. Diagram of Quantitative Reservoir Characterization

Furthermore, the results of simultaneous inversion consist of acoustic impedance, shear impedance, and density will be used as the input for porosity and saturation inversion. The inversion was done only on specific section where it has high probability as derived from probability classification cube (qualitative characterization). Output of this process will be estimated model of porosity and saturation.

2.2 Biot-Gassmann Theory

In an isotropic rock formation, a sedimentary rock can be characterized by their bulk modulus, shear modulus, and density. When seismic wave passes through formation, their propagation not only depends on their elastic properties, but also depends on porosity and fluid saturation in the formations. A rock which loaded under an increment of compression will have change in pore pressure; this will resist the compression and therefore stiffens the rock (Mavko et al., 1998). One of general formulation of wave propagation in porous is explained by Gassmann (1951) – Biot (1956). The equation is only dealing with bulk moduli, shear moduli, and density which can be described in two equations as follow,

$$\frac{K_{sat}}{K_0 - K_{sat}} = \frac{K_{dry}}{K_0 - K_{dry}} + \frac{K_{fluid}}{\phi(K_0 - K_{fluid})} \quad (2.1)$$

$$\mu_{sat} = \mu_{dry} \quad (2.2)$$

Where,

K_{dry} = effective bulk modulus of dry rock

K_{sat} = effective bulk modulus of the rock with pore fluid

K_0 = bulk modulus of mineral making up rock

K_{fluid} = bulk modulus of pore fluid

Φ = porosity

μ_{dry} = effective shear modulus of dry rock

μ_{sat} = effective shear modulus of rock with pore fluid

From equation 2.1 and 2.2 above, it can be seen that fluid in porous rock will affect bulk moduli. However the presence of fluid or no presence of fluid does not affect the shear modulus. Indirectly, this means that fluid does not alter rock solid matrix properties. Thus, it can be seen that the practical aspect of Biot-Gassmann theory is to predict one condition of fluid from another in a sedimentary rock. For example, if we have dry well containing water in pore space, and we measured the compressional velocity, shear velocity, and density. We can predict the behavior of this well if the pore space was occupied by gas, by transforming the first condition (wet) to dry state, and then immediately transform the moduli to the

new saturated state. By doing this wet zones or hydrocarbon zones are able to be clustered in well condition

Biot-Gassmann by theory is valid on sufficiently low frequencies. This low frequency type is in situ seismic data (< 100 Hz), because Biot-Gassmann theory assumes a homogenous mineral modulus and statistical isotropy of pore space, with no assumption about pore geometry (Mavko et al., 1998).

Since this theory does not dealing with pore geometry specific, there are some potential pitfalls in applying Biot-Gassmann theory in carbonate sedimentary rocks. Due to heterogeneity in carbonate, Biot-Gassmann failed to predict shear moduli. Baechle (2005) reported their laboratory measurement on dry and wet conditions which show the shear modulus does not remain constant during saturation, which failed equation 2.2. They suspected that the variability occurred due to interaction between rock and fluid, and due the pore type variation at any given porosity. This kind of heterogeneity existed due to significant geochemical mobility of carbonate minerals which created complex cementation/dissolution patterns in carbonate rocks, and sometimes the elements had their own porous structure (Rasolofosaon et al., 2008). Another recent laboratory measurement done on carbonate samples by Adam (2006) showed that at high differential pressures and seismic frequencies, the bulk modulus of rocks with high-aspect-ratio pores and dolomite mineralogy is predicted by Gassmann's relation, and also rock shear modulus in the carbonate sample change from dry to brine saturation conditions. Even though, question still remain unanswered with fluid modeling in carbonate sedimentary rocks, I would assume locally in my area of study, Gassmann equation will apply in certain condition.

2.1.1. Velocity-Porosity & Saturation Analysis

One of the objectives in this thesis is to qualitatively characterize the porosity of the carbonate and the water saturation distribution. In previous section, forward modeling of elastic moduli such as bulk modulus, shear modulus, and density as a function of porosity and fluid saturation using Biot-Gassmann relationship was

discussed. It indirectly concludes that if we want to estimate porosity and saturation from velocity (seismic), we need to determine two variables (porosity and saturation) and perform a joint estimation problem (Bhachrach, 2006). The uncertainty in porosity estimation leads to uncertainty in saturation estimation.

There are many deterministic solutions in estimating porosity and saturation from seismic velocity or vice versa. Nevertheless, sometimes the direct transformation is too optimistic. Mavko et al. (1998) explains that, if we wish to predict effective elastic moduli of a mixture of grains and pores theoretically, we generally need to specify (1) volume fractions of various phases, (2) elastic moduli of various phases, (3) geometric details on how the phases are arranged relative to the others. If we only know about volume fractions and constituent moduli solely, what we can do, is predicting the upper bound and lower bounds. We can predict at any given volume fraction of constituents the effective modulus will fall between upper bound and lower bound, known as Hashin-Shtrikman Bounds as illustrated below,

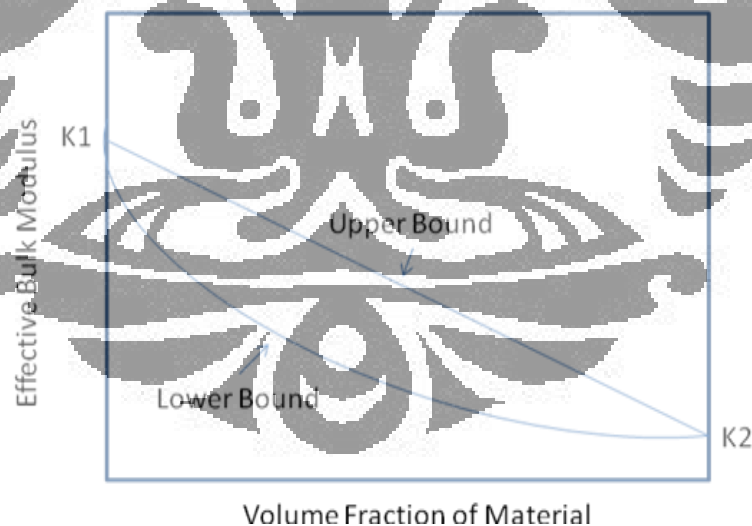


Figure 2.3. Hashin-Shtrikman Bounds

In this thesis, joint porosity-saturation inversion via stochastic modeling and Bayesian theory was conducted. The Biot-Gassmann theory constrained the rock physics modeling by relating seismic velocities to porosity and saturation. All

ranges of porosities and saturation were explored, and then simulate the sediment clastic response associated with the rock physics forward models using stochastic modeling. In the end, we will realize a range of posterior probability value from this calculation using Bayesian theorem, and then find the associated value representing minimum error between forward modeled data and measured data as the solution. Detailed explanation of Bayesian theorem will be explained in the next sub-chapter.

2.3 Simultaneous Seismic Inversion

In recent decades, there has been significant improvement in seismic based reservoir characterization research. This was triggered by the applicability and the promising result in applying the method for commercial situation. One of the popular methods nowadays is the employment of partial angle stack into the same inversion kernel to produce elastic attribute such as acoustic impedance, V_p/V_s ratio and density.

Successful introduction of post-stack seismic inversion to produce acoustic impedance makes seismic data more geologically sounds because acoustic impedance correlated with lithology. People try to explore the possibility of extracting fluid information from seismic data. Using shear wave (S-waves), we can detect fluid content within reservoir, because compressional waves (P-waves) is sensitive to changes in pore fluid and S-waves is related with the interaction with the rock matrix. This particular pre-stack seismic inversion data can be significantly useful for lithology and fluid discrimination. In pre-stack seismic data, we can extract shear wave information which was contained within the variation of reflection coefficient with source-receiver offset (AVO).

2.2.1. Aki-Richards Equations

The ability to deduct sub-surface physical information from seismic waves comes from the fact that each lithology contrast has different behavior when disturbed by seismic waves (Munadi, 2000). In seismology, the reflection and transmission behavior of seismic waves in boundary has been formulated by many scientists, one of the notable formulas is the Knott-Zoepprits equation. That is a highly non-

linear and complex equation. Recently many scientists proposed simplification to Zoepprits equation, one of them is Aki-Richards equation (1980), which was explained in Munadi (2000),

$$R(\theta) = \frac{1}{2} \left(1 - 4 \frac{V_s^2}{V_p^2} \sin^2 \theta \right) \frac{\Delta \rho}{\rho} + \frac{1}{2 \cos^2 \theta} \frac{\Delta V_p}{V_p} - 4 \frac{V_s^2}{V_p^2} \sin^2 \theta \frac{\Delta V_s}{V_s} \quad (2.3)$$

In this case,

V_p is average velocity for P wave from layer below and above the interface

V_s is average velocity for S wave from layer below and above the interface

ΔV_p , ΔV_s , $\Delta \rho$ respectively is P wave velocity contrast, S wave velocity contrast, and density velocity contrast

Using Aki-Richards equation above, relationship between reflectivity series as a function of angle (in other name AVO, amplitude variations with offset) with V_p , V_s , and density can be established. We acquired and obtained the reflectivity series of sub-surface using seismic reflection method, therefore problematic of extracting V_p , V_s , and density from seismic data is an inversion modeling issue. This can be solved by partially inverting each angle stack or simultaneously using all angle stacks in one inversion scheme. In the diagram below (figure 2.4) shows the comparison in separated AVO inversion scheme and simultaneous AVO inversion scheme.

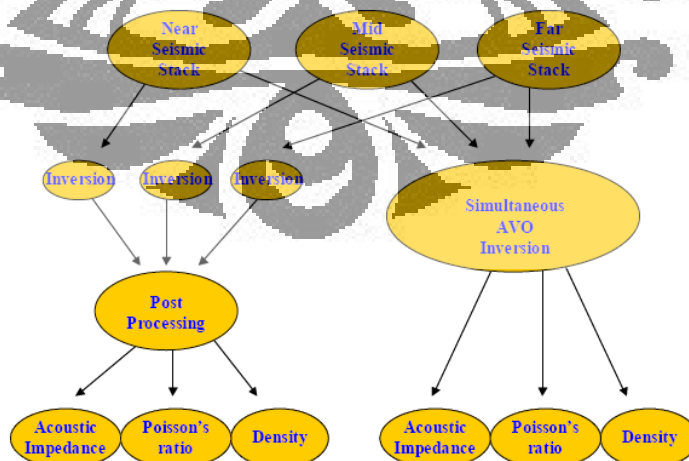


Figure 2.4. Comparison between separate inversion and Simultaneous inversion (Maver, 2004)

One of the first achievements in extracting shear wave information from AVO data was done by Connolly (1999), as illustrated in figure above; each angle stack was inverted in separate inversion kernel. Each inversion process then produces elastic impedance from each angle stack, post inversion processing then carried to extract acoustic impedance, Poisson's ratio, and density. This method was latter known as separate inversion method. It is noticed that combining multiple frequency content of partial stacks into separate inversion process lead to potential disadvantages. Since far offset data will contain lower frequencies due to attenuation and NMO stretch, there will be potential noise when combining different frequency content on the estimation of angle independent quantities.

Utilizing single inversion kernel for inverting partial seismic stack has an advantage over separate inversion process. This method is widely known as simultaneous AVO inversion method. Using this method, all of the angle stacks was inverted using the same inversion kernel. The elastic attributes such as acoustic impedance, V_p/V_s ratio, and density were inverted directly without any post inversion processing. Thus, there is no need to integrate multiple angle stack data. Further advantages of simultaneous inversion over separate inversion have been reported widely, some of them are Ma (2002) and Maver (2004).

In this thesis, simultaneous seismic inversion algorithm based on simulated annealing (Ma, 2002) was used; this method is commercially available in Schlumberger Oedegaard-ISIS software (Maver, 2004). In the algorithm, Ma (2002) combined the AVO extraction and impedance inversion into a single step, and formulates it as a global optimization problem. The optimization procedure adapts the simultaneous annealing algorithm, allowing flexible constraints to be built in. The global optimization technique will enhance the inversion process in order not to trap in local minima. Trace by trace continuity also introduced into the algorithm, this will help to suppress the noise.

The algorithm works by inverting partial angle stacks using specific wavelet for each angle stack. Independent wavelet for each stack will handle any variation in

amplitude, frequency, and phase between the different seismic volumes. Inversion itself will be performed directly for physical properties of interest; this can be acoustic impedance, shear impedance, V_p/V_s ratio, and density.

To compensate lack of low frequency information from seismic data, the algorithm required prior low frequency model. This model can be built by interpolating well logs value with the horizons, introducing low frequency guidance from seismic velocities, and giving information about depth trend of geology. Furthermore, inverse problem is a non-unique problem, without constrain there may be a lot of solution with different low-frequency trends that satisfy the inversion result. This low frequency model will act as inversion constrain.

Elastic information for each trace positions were extracted using simultaneous seismic inversion method. This is the input to map fluid information from well log into 3D space. Since Bayesian is just another statistical process, the accuracy of seismic inversion that calibrated by measured well information is needed.

2.4 Bayesian Theorem

Bayesian theorem in short understanding can be viewed as conditional probabilistic. Munadi (2005) pointed out that Bayesian theorem provides mathematical formulation to handle how a probability can be revised if there is new information available. In a previous research done by Murdianto (2007), he showed how to do reservoir characterization using Bayesian theorem, by integrating Bayesian theorem to constrain facies simulation.

The theorem itself stated if we have two events x and y , we can design the probability of occurrence of each event by $P(x)$ and $P(y)$. If we consider of the probability of this two events, we can designed this as joint probability of $P(x,y)$ that is given by,

$$P(x, y) = P(x | y)P(y) = P(y | x)P(x) \quad (2.4)$$

In this case, $P(x/y)$ is the probability of x to occur given that y already occurred, the same situation applied to $P(y/x)$. Therefore $P(x/y)$ and $P(y/x)$ can be defined as conditional probabilistic. From equation 3, if we want to know how the probability of y is, given x already happened, we can re-arrange the equation into,

$$P(y | x) = \frac{P(x | y)P(y)}{P(x)} \quad (2.5)$$

The term $P(y/x)$ is the probability of event that we want to know given x condition, this term defined as *posterior probability density function (posterior PDF)*. It is the condition where we can say how the probability of a model is correct given a set of information. The second term that holds the fundamental of Bayesian theorem is the *likelihood function*, $P(x|y)$. Murdianto (2005) stated this is the PDF which associated with possible realization of a particular parameter. The third term that builds the fundamental of Bayesian theorem is the $P(y)$, this is called *prior* PDF of y to be happened that does not take into account any information about x . This is initial *a priori* information or initial knowledge that we have about a certain parameter. And then $P(x)$ is the prior probability or marginal probability of x to be happened. To complete equation 5, according to the total law of probability, since,

$$P(x) = P(x | y)P(y) + P(x | y^c)P(y^c) \quad (2.6)$$

In equation 2.6 above, $P(y^c)$ is defined is probability of not having y to be happened. Therefore the complete Bayesian equitation to defined conditional probability of y to be happened given x that already happened is,

$$P(y | x) = \frac{P(x | y)P(y)}{P(x | y)P(x) + P(x | y^c)P(y^c)} \quad (2.7)$$

For example, suppose there is a distribution of acoustic impedance (AI) having 50% chance of shale and sand as lithology. Sand has 30% chances to be high AI, and 70% chances to be low AI. And shale has 80% chances to be high AI. A new

data was given, it is a high AI. What is the probability that this new data is sand? This can be answered using Bayesian theorem.

- $P(y)$ = the probability of sand, regardless of any information = 0,5
- $P(y^C) = P(x)$ = the probability of shale, regardless of any information = 0,5
- $P(x|y)$ = the probability of lithology is high AI given the lithology is sand = 0,3
- $P(x|y^C)$ = the probability of lithology is high AI given the lithology is shale, = 0,8

Therefore using equation 7, where the probability of sand given the new data is high AI, $P(y|x)$ is 0,38. If no a priori information has been known, probability for all hypotheses will be distributed evenly to all hypotheses. This was used in the example above, where if we do not know how the sand and shale distribution in the data, we set 50% prior probability for sand and shale. The Bayes theorem will update the knowledge after new data has been observed.

The product of Bayesian calculation is posterior PDF from each alternatives, sometimes this is not a practical way to representing the result of Bayesian calculation. A representative value commonly used to define this result is Maximum a Posteriori (MAP) is the optimal representative value with the posterior PDF. In Bayes estimation, MAP minimizes the Bayes risk, and is optimal in the sense that it reduces the uncertainty associated with prediction of value. Maximum a posterior simply defined as mode of posterior PDF. Given sets of data x , the maximum a posterior to form hypothesis h can be defined,

$$h_{MAP} = \arg \max P(h | x) \quad (2.8)$$

One of the simplest forms of Bayesian classification is the naive Bayes classification. In this classification, it was assumed that given an output number, total probability from all observations are product of each individual observation and its independent of each other (Santosa, 2007).

For most of the cases, decision making or classification will be based on sets of observation. The lithology or fluid classification in this study for example, will use two sets of observation. They are observation on variability in the acoustic impedance and the variability in Vp/Vs ratio. There will be no interdependency between acoustic impedance and Vp/Vs ratio in naive classification, even though acoustic impedance may get affected by Vp/Vs ratio.

Inverse problem can also be solved using Bayesian theorem. If we recall the Bayesian in equation 5, this can be re-written to be,

$$P(m|d) = \frac{P(d|m)P(m)}{P(d)} \quad (2.9)$$

In equation 2.10, d and m denote data and model. Posterior probability which represented by conditional probability for the model given data, $P(m/d)$, is the solution of inverse problem (Grandis, 2002). Stochastic simulation will be performed using large number of data to generate joint probability of porosity and saturation. Therefore using Bayesian theorem, the posterior probability which in fact is the solution of inverse problem will have its own measurement of confidence and measurement for each model. Maximum a posterior analysis will be used to define most fit model to data.

CHAPTER 3

PETROPHYSICS AND BASIC ROCK PHYSIC ANALYSIS

Well log data measures directly in-situ reservoir properties. They have good degree of depth resolution (or vertical resolution), but low degree of coverage (spatial coverage). However, detailed understanding of elastic attribute in measured well log data is the fundamental part in seismic inversion and attribute mapping based on seismic inversion. In this chapter we will begin the modeling analysis based on formation evaluation/ petrophysical analysis from AGR-1 and then followed by cross plotting of elastic attributes to define fluid classes. The fluid effect on velocity was analyzed by doing fluid substitution on AGR-1 using Biot-Gassmann theory. Synthetic seismic gather was also generated as comparison with surface seismic data.

3.1. Petrophysical Analysis

In the study area, we only have 1 well. This is a discovery well, where substantial amount of gas has been found within Kujung-I carbonate interval. Besides standard open hole logs (gamma ray, resistivity, porosity, and density), dipole sonic imager also was run in this well to get compressional sonic and shear sonic data.

There are 4 major formation tops in AGR-1, these are Kujung-I, GWC, Kujung-II, and Basement. Formation evaluation was done from various wells information. The analyses start by doing log correction, Vshale computation using thorium GR. The zones were defined while doing the Vshale computation; this was done by analyzing typical gamma ray responses. Formation evaluation analysis concluded that the hydrocarbon was placed above gas water contact (GWC), this was based on deterministic analysis and Pickett plot at GWC zone. The well was tested, the result show that possible gas water contact at depth 2652 ft TVDSS. Water zone was confirmed with LFA (live fluid analyzer) and pressure gradient. As a conclusion, we defined the cut off to get the pay zone, these are Vshale in net

reservoir is less than 40%, the effective porosity is above 10 %, and water saturation below 65%. The result of the petrophysical analysis is shown below, and the zone of interest is marked with yellow circle,

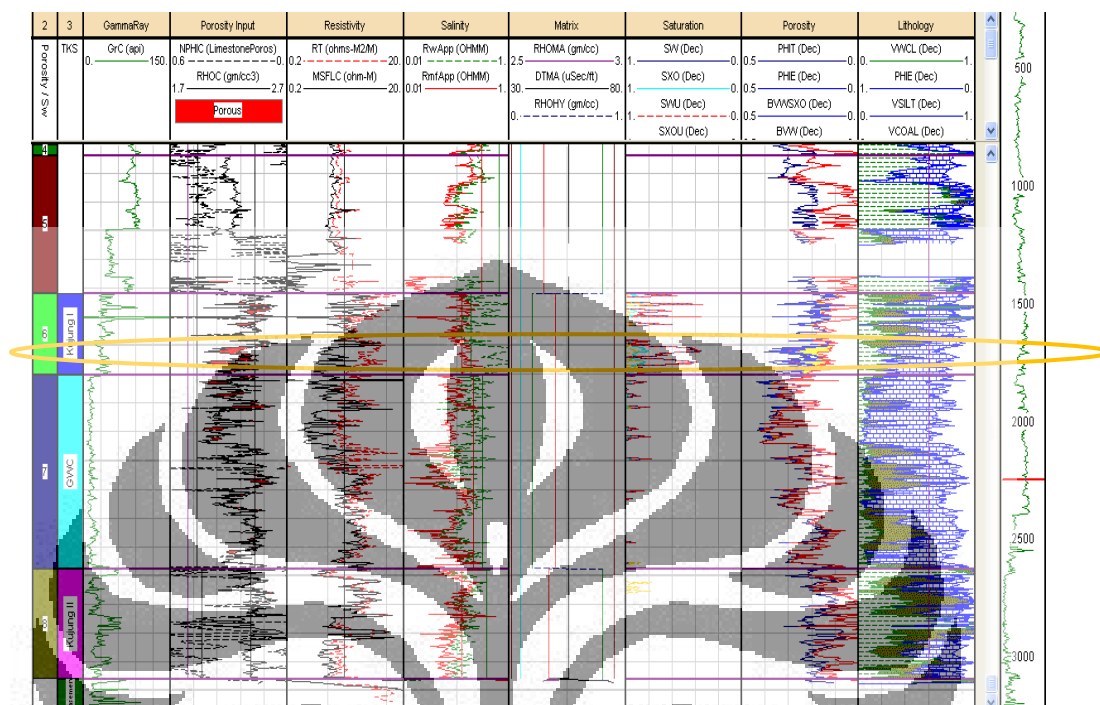


Figure 3.1. Petrophysical analysis of AGR-1 (Pearl Energy Internal Report, 2009), zone of interest marked with yellow circle.

From this petrophysical analysis, two fluid classes were defined. They are Kujung-I gas filled carbonate, Kujung-I wet or water filled carbonate. The zone of interest was slightly above GWC. Even though, zone slightly below Kujung-I show less water saturation, this zone was tested to be a tight zone.

3.2. Fluid Replacement Modeling

Main objective of fluid replacement modeling is to see the effect of fluid on measured log (velocity) data. In this well, the gas occupied Kujung-I porous zone with water saturation around 40%-60%, the observation shows this zone can be identified by drop in V_p/V_s ratio. Figure below shows cross plot of acoustic impedance versus V_p/V_s ratio with water saturation as color scale only at Kujung-I to Basement interval.

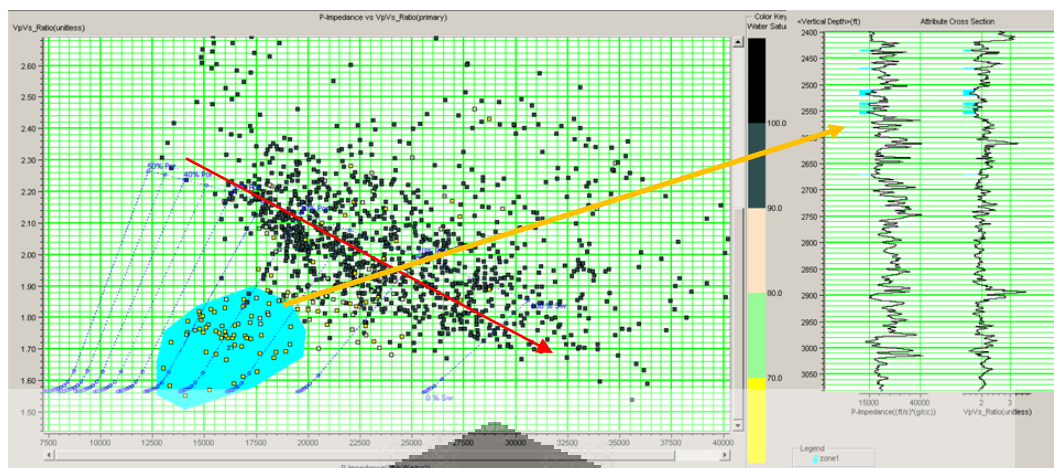


Figure 3.2. Crossplot AI vs Vp/Vs vs Sw over Kujung Interval

Data distribution is scattered, interpreted as common thing for carbonate. Observation on cyan polygon above, it can be noticed that a low water saturation zone correlated with our Kujung-1 reservoir. It was also observed the wet trend zone pointed by red arrow. Initial conclusion by looking at this cross plot is Vp/Vs ratio can be used as indicator of gas and wet zone.

Analyses of velocity behavior when the porous zone occupied by 100% water and 100% gas were done, that is the fluid substitution exercise. The objective of this exercise is to see the extreme separation in AI vs Vp/Vs ratio distribution, and observe the distinct behavior in elastic attributes. The analyses were done using Biot-Gassmann theory to do fluid substitution exercise within Kujung formation only. The rock matrix was defined from two minerals, one is clay where the volume fraction derived from petrophysical analysis and the other is calcite, where the volume is adjusted to 100%. The hydrocarbon is defined as gas where the bulk modulus is 0.021 GPa and density is 0.1 g/cc. Brine's bulk modulus defined as 2.38 GPa and density of 1.09 g/cc. First the porous zone was substituted to 100% water, which previously was occupied by gas.

In Figure 3.2 above, there is a blue dashed line. This is rock physics template derived from Biot-Gassmann theory for each 10% increase in porosity. The wet trend line fall on 100% water saturation, and our reservoir fall in 25-40% porosity

with approximately 40% water saturation, as analyzed by petrophysical formation evaluation.

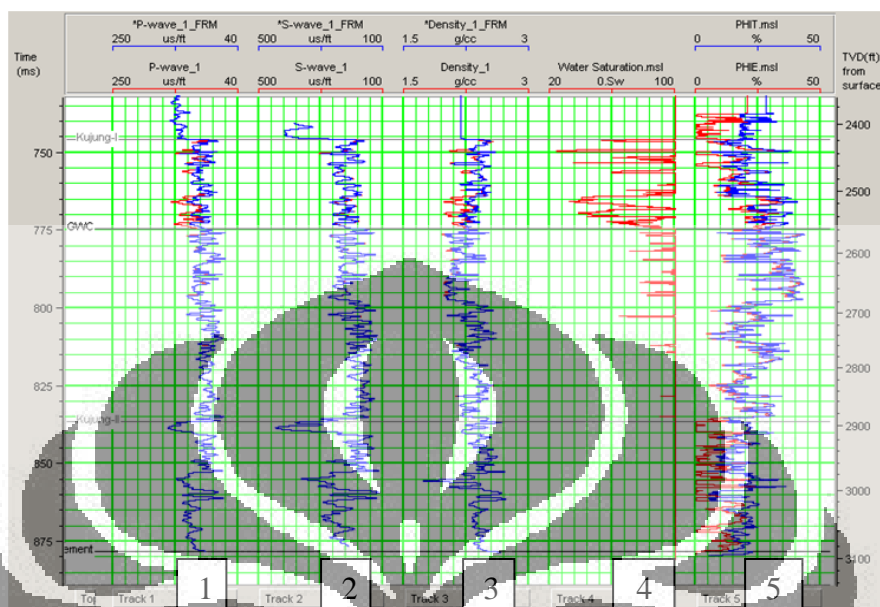


Figure 3.3. Elastic Log after Substituted to 100% water (red is in situ measured log, blue after substituted to 100% water)

In panel 1 from figure 3.3 above, the blue curve is compressional sonic log after fluid substitution, and red is measured compressional sonic log. Zone above GWC was obviously defined as gas zone, where it were noticed in petrophysical analysis and well test, and also by dropping in compressional sonic log, the zone below GWC is water as previously defined in formation evaluation. When the porous zone substituted to be 100% water, it is expected the compressional sonic log to fall in alignment with sonic from water zone. Density will be affected by this process, but not shear sonic as mentioned by Biot-Gassmann theory assumption. It is interpreted that Biot-Gassmann theory is working as expected in carbonate sedimentary rock in this area. This conclusion was deduced by the fact, sonic log after substituted to 100% water falls into alignment with measured sonic in water zone. For sure, this is local conclusion and not fully supported with a lot of facts. In this particular exercise, the objective to define zone where 100% gas and 100% water is achieved just by using Biot-Gassmann theory.

3.3. Synthetic AVO Modeling

It is a good exercise to compare synthetic seismic gather with measured seismic gather, one of the advantage of doing this is to maintain our expectation on seismic inversion result. Within this sub-section, synthetic seismic gather were computed for in-situ reservoir condition (gas), and reservoir condition where we have 100% water in the porous zone. The reflectivity was calculated using Aki-Richards equation, and synthetic seismic trace produced by convoluting the reflectivity using 20 Hz zero phase ricker wavelet for simplicity.

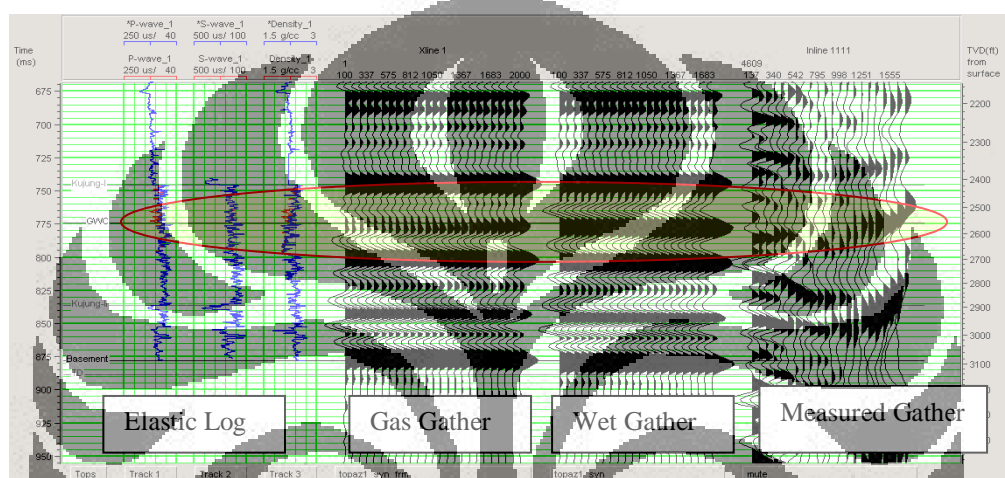


Figure 3.4. Synthetic Gather Modeling

The amplitude variation with offset was observed in GWC, spotting the interface for base gas zone in Kujung-I with the water zone below it, marked with red circle. If the well is occupied by water then there will be no amplitude variation with offset. Comparing these two gathers help to determine what kind of AVO characteristic to distinguish between gas and water. The measured gather that is still *very raw* gather after migration, without any further processing cosmetic except stretch mute. It is observed there is no good correlation between synthetic and measured, this suspected due to mismatch in wavelet and the measured gather needs further processing.

In figure 3.4, the measured seismic shows event above 1200 ft offset is not perfectly flattened. This may lead to imperfect density extraction within inversion algorithm. An explanation that can be drawn with this phenomenon is because of the effect of anisotropy that didn't take care of in the velocity analysis.

3.4. Velocity-Porosity Relationship Analysis

Besides qualitative classification, the purpose of this study is to do quantification of carbonate reservoir in terms of their porosity and saturation. This will be done by applying stochastic modeling to jointly estimate porosity and saturation.

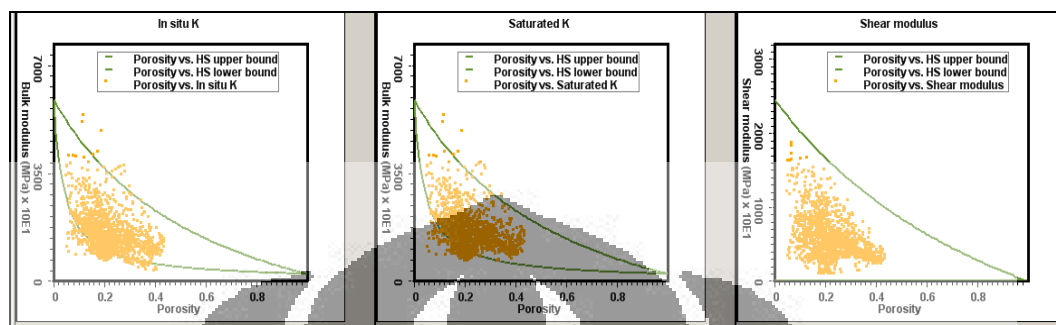


Figure 3.5. Porosity-Elastic Moduli Relationship

Figure 3.5 above is the cross plot between bulk modulus and porosity from measured well log data. Upper bound and lower bound of Hashin-Shtrikman were defined using two mineral models (clay and calcite). The same brine and hydrocarbon properties with fluid replacement modeling were used. Unfortunately the mineral model from petrophysicist needs to be checked further, since there is still anomalous point outside upper bound and lower bound. The model needs to revise further for fluid (brine and hydrocarbon) modulus and density estimation. Valuable information that observed is, the data distribution tend to fall on lower bound. Based on rock physics theory (Mavko, 1998), this can be roughly interpreted as Kujung-I have softer pore shapes. Correlation of this feature with Adam (2006) publication and the fact that the prediction of wet condition in fluid replacement modeling is quite good, Kujung-I carbonate may have high-aspect-ratio and softer pore shapes. The answer to the question of how porosity and saturation can be estimated will be based on this model, since stochastic modeling will extrapolate/simulate based on this model.

CHAPTER 4

SIMULTANEOUS SEISMIC INVERSION

To map rock information from measured well logs in 3D space, it is needed to invert surface seismic amplitude to elastic attributes and before mapping it with Bayesian theorem. Within this chapter, the analysis on simultaneous seismic inversion that was performed to get elastic attribute from study area was explained. The analysis will cover data conditioning prior to inversion, log calibration and wavelet extraction, low frequency model building, and inversion.

4.1. Angle Stack Alignment

Simultaneous seismic inversion is dealing with multiple seismic volumes that measured same geological feature. Ideally, all the seismic signals will capture subsurface geology and image the same physical interval without any difference among all angle stacks. However, some event misalignment could still happened in place. This may be due to processing artifacts, different frequency content, or some other things. The inversion result will be affected by these misalignments.

In this exercise, the angle stack alignment was done by time-shifting one volume using specific time-shift to match the reference volume. This time-shift was estimated from 1-D cross correlation within specific time window between volumes and its reference volume. This study used three angle stacks (near, mid, and far) as inversion input, mid angle was selected as the reference. Based on understanding that the alignment will perform time shifting on initial volume and it is not expected to shift radically the volume that could possibly change the information inside the angle stack. Alignment of far angle stack to near angle stack will change the far angle stack radically, rather than alignment of far angle stack to mid angle stack. Because far angle stack is expected not to have big variation in frequency content compare to mid angle stack. It will be unwise to force far stack to match near angle stack. Therefore, the workflows were alignments of near angle stack to mid angle stack, and far angle stack to mid angle stack.

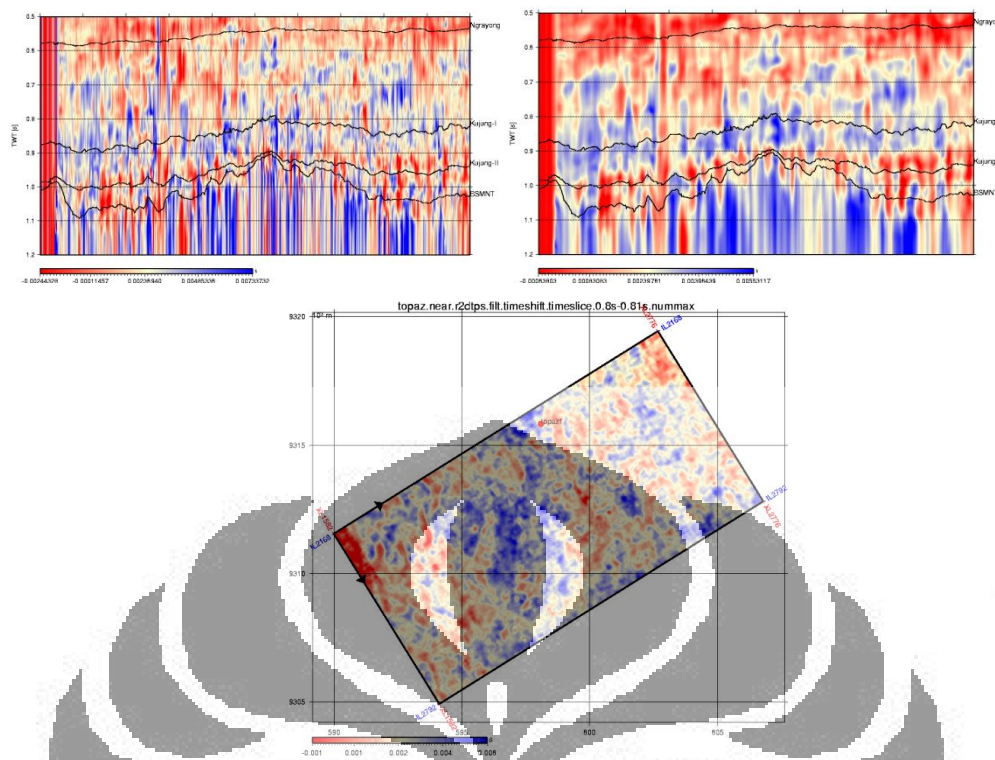


Figure 4.1. Alignment in one In-line on near to mid alignment, without filtering (top-left) with horizontal filtering (top-right). Lateral time-shift map (bottom)

One dimensional cross correlation will have disadvantage when there is bad trace. Besides that, this time-shift calculation based on 1-D cross correlation was not conformed and took into account any geological information. Horizontal filtering was performed on estimated 1-D time-shift based on interpreted horizons. By doing this, the bias due to bad traces was minimized and consistently conformed time shift based on geological horizons among all angle stacks. Difference in frequency content between angle stacks can also affect time-shift estimation. Inside the process, frequency balancing between two volumes was performed prior to time-shift estimation, thus, the cross correlation was performed in the same condition. However, the frequency balanced volume was not shifted as result of this exercise, the time-shift alignment applied on initial volume. Figure 4.1 above shows comparison before horizontal filtering (top-left) and after horizontal filtering (top-right). Those QC plots are intended to check whether there are anomalous time-shift values. The bottom figure shows time-shift in lateral manner showing no anomalous time-shift.

4.2. Log Calibration and Wavelet Extraction

Wavelet is the key to inversion process. The wavelet shape affects the inversion result significantly, so this is a critical step to produce reliable inversion result. Wavelet extraction performed the extraction in time domain using least square method. In this method, both wavelet amplitude and phase spectrum are derived from the correlation in time domain between seismic data and well log data. The least square method minimizes the sum of squared misfit between seismic trace and synthetic trace obtained by convolution of well log reflectivity series and wavelet. A series of wavelet length and initial delay will be extracted; the optimum wavelet will be picked by finding the minimum misfit. In this exercise, simultaneous inversion will use Aki & Richards AVO reflectivity model.

It has been informed that the processing did not shape the data to specific phase. Initial extraction showed the data is not perfectly zero phases. Well seismic tie was performed using acquired checkshot data in this well. However, checkshot itself was not sufficient enough to produce good wavelet since there was still a mismatch and poor correlation between synthetic log with seismic trace, visual tie needed to match seismic with synthetic. A constant bulk shift average of 10 ms for event close to Kujung-I was applied to get good correlation.

The wavelet was extracted within the target zone (Kujung-I to Basement or ~0.7-1.0 seconds), within this window the spectrum of the wavelet was defined using previously explained method. An Average of 80% correlation observed between synthetic seismogram and surface seismic. The phase was controlled using defined constant phase. Figure 4.2 below, shows the correlation between synthetic seismogram with surface seismic. The synthetic seismogram was computed for each angle stack using specific extracted wavelet. At the zone of interest (circled in yellow), shows good correlation in terms of event correlation and amplitude correlation.

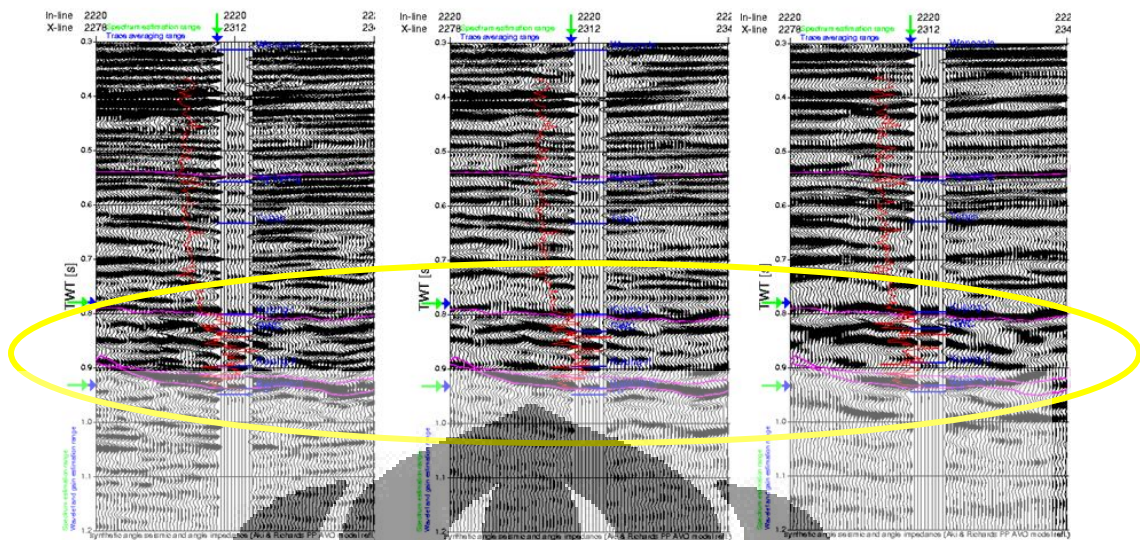


Figure 4.2. Synthetic seismogram inserted into each angle stack (near-left, mid-middle, far-right) shows good correlation on zone of interest.

To get a good wavelet, initial knowledge about data processing is highly required. Any kind of wavelet can be extracted and have good correlation with surface seismic without any geological information, if it forced to be like that. Good wavelet will be defined whenever the event in well log tied right at the proper seismic event. Normally the quality control of extracted wavelet was using statistical correlation between synthetic seismogram and surface seismic, another good quality control is to check whether wavelet can model the surface seismic amplitude. Figure 4.3 below is quality control plot of how the wavelet can model the surface seismic frequency spectrum in the target zone. In all near, mid, angle wavelet stacks, it is concluded that the wavelet can modeled the surface seismic spectrum.

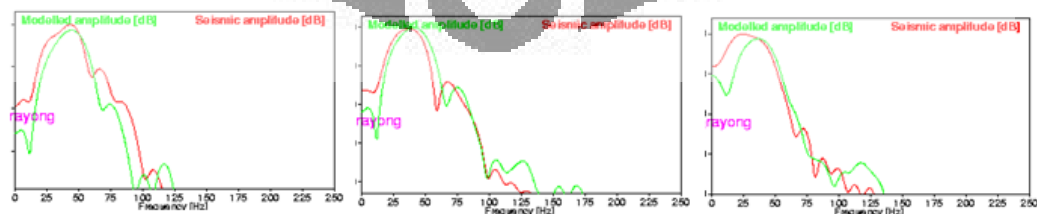


Figure 4.3. Comparison of measured seismic amplitude with modeled amplitude using extracted wavelet for near (left), mid (middle), and far (right)

Figure 4.4 below shows the summary of extracted wavelet. All the wavelets show expected shape, where the far angle wavelet (red line) is broader due to lower frequency, and near angle (blue dotted line) is narrower due to higher frequency. Wavelets phase are almost consistent throughout all the angle stacks, increasing confidence in seismic inversion process.

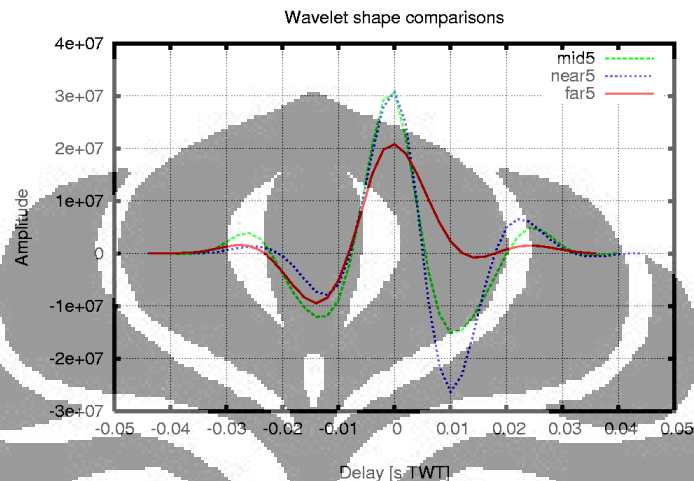


Figure 4.4. Summary of extracted wavelet

4.3. Low Frequency Modeling

Seismic data is band limited; they are missing low frequency band. This missing information is related to geological feature. In the other hand, well log data has wider frequency band. Integrating the two of them will provide inversion result with geological information from well log low frequency content, and high frequency information which contain detailed subsurface feature from surface seismic. One way to integrate these two information is by interpolating well log value with interpreted horizons. This will be the starting model, or the prior model for inversion. Another way to give geological feature to inversion result as in structural information is introducing layer sequence field and dip sequence field to prior model. Layer's dip can be estimated using numerical formulation by finding gradient between horizontal distance (offset) and vertical distance (vertical time). On top of that, careful and detailed quality control and validation of the log calibration (well to seismic tie) are needed, since the interpolation will be based on this exercise.

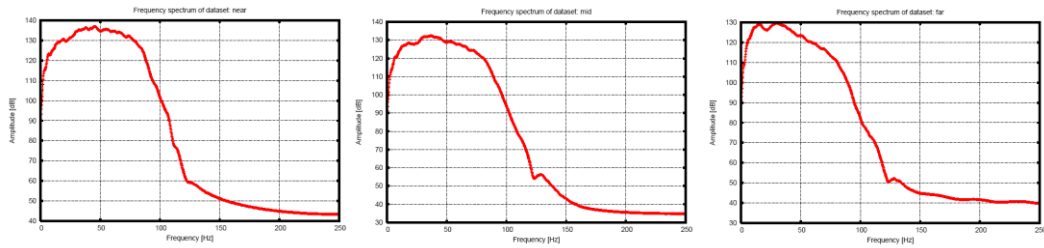


Figure 4.5. Frequency content of near (left), mid (center), far (right) stack

In this low frequency modeling exercise, there are 4 interpreted horizons available; Ngrayong, Kujung-I, Kujung-II, and Basement. All of them were used in the interpolation of well logs value. Layer sequence field was used to help guiding the structural information. Analyses on the frequency spectrum from all angle stacks (see figure 4.5 above), show the missing frequency are below 10 Hz. In the process, full spectrum was interpolated from well log to 3D cube, and then low filtered with high cut of 10 Hz. Comparison of low pass filtered well log with measured well log is shown in figure 4.6. This figure show comparison between low pass filtered acoustic impedance, Vp/Vs ratio, and density low frequency with their respective measured log responses.

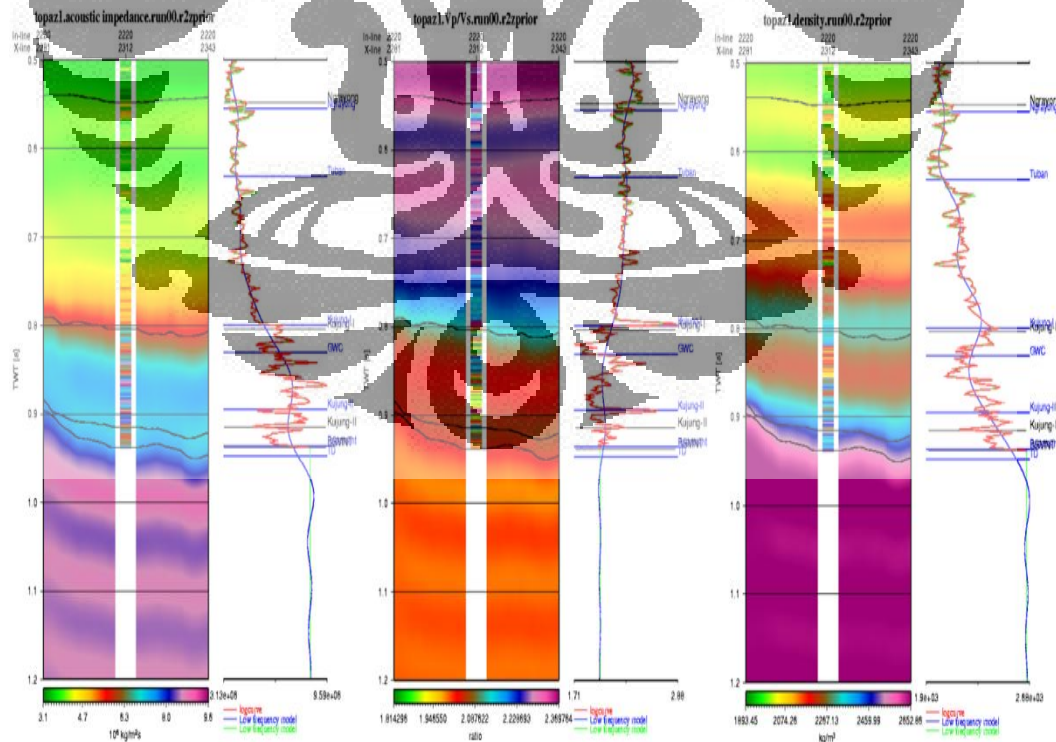


Figure 4.6. Low Frequency Model for AI (left), Vp/Vs Ratio (middle), and density (right)

Other workflow that can be done to build reasonable quality of low frequency model is using the surface seismic migration velocity. If good migration velocity available, this velocity can be transformed into impedance and provide low frequency information throughout our cube. Based on internal discussion, sometimes this surface seismic velocity can provide low frequency information down to 3 Hz. Due to different burial sedimentation rate, sometimes some area has different compaction trend or depth trend compared to other area. This interpreted as, within the same layer, the acoustic impedance does not have the same value because the difference in burial sedimentation rate. Estimation of depth trend can be extracted from well log low frequency trend, and can be useful if there is more than one well log available. We suggest for in the next research to build more sophisticated low frequency model by employing surface seismic velocity and depth trend.

4.4. Inversion

The inversion was done using low frequency model as a starting model. Inversion algorithm was performed to extract three elastic attributes: acoustic impedance, V_p/V_s ratio, and density. In the starting model, prior model of acoustic impedance, V_p/V_s ratio, and density low frequency model were defined respectively. A global optimization technique (simulated annealing) is used in order to make the inversion not to get trapped in local minimum models close to starting model. The forward modeling within inversion algorithm was done by convolutional model using Aki-Richards reflectivity model, the same model that was used in wavelet extraction method.

There are three important parameters that control the inversion,

- Standard Deviation from Low Frequency Model
This parameter control how far the inversion can deviate from starting model.
- Horizontal Continuity

This is used to control horizontal variation in the estimated inversion result. The global optimization technique is employed multi trace calculation; it is needed to set reasonable degree of horizontal variation.

- Reflector significant level

This is a degree of presence of significant reflectors. The reflector will be placed in estimated inversion result if the reflection coefficient exceeds this threshold.

Previously in the log calibration and wavelet extraction process, the correlation was optimized within target zone, which is between Kujung-I and Basement. The inversion result showed promising results; even though in the rest of the zone is not as good as in target zone. Figure 4.7 showed the acoustic impedance (AI) result. In simultaneous seismic inversion, AI is one of the easiest parameter to extract. The blue curve in the figure shows the inversion result; meanwhile red curve is the measured log response. It is observed especially in zone of interest (0.8 s to 1.0 s), the inverted trace (blue curve) is matching the measured log response quite well. The zone above 0.8 seconds was poorly inverted because of poor correlation, also the zone below 1.0 seconds was poorly inverted because of lack low frequency model constrain that was based on well log interpolation using seismic horizon.

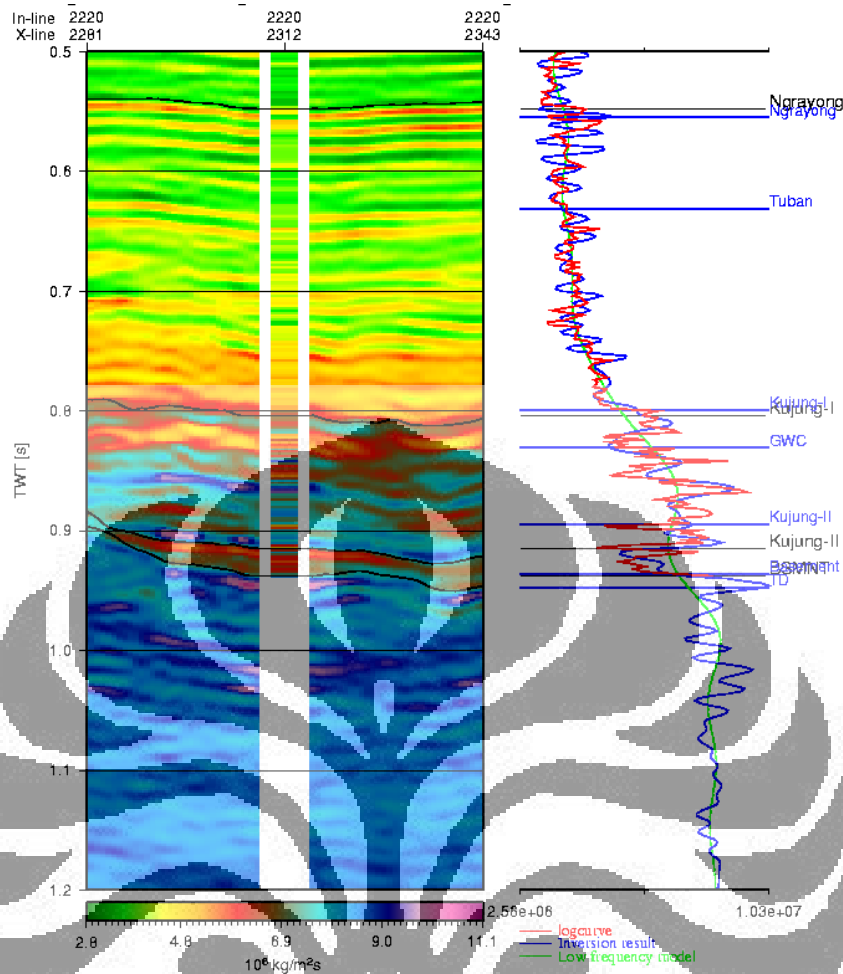


Figure 4.7. AI Inversion result and it's comparison with measured AI

Second attribute that was extracted is the V_p/V_s ratio, the QC plot is shown in figure 4.8. Shear wave information was derived based on variation in amplitude against the offset. The quality of mid and angle stacks will contribute to shear information extraction. Challenges on optimizing non-linear parameter also come in place. All of these challenges make V_p/V_s inversion result a bit deviated in expected quality compare to AI inversion result. However, the inversion was catching up the well log variation in a reasonable result. The gas in the target zone was inverted as expected. The poor inversion result above Kujung-I (0.5-0.8 s) was because poor synthesis of the shear log. The Schlumberger Dipole Sonic Log was only logged within target zone. Imperfect synthetic shear log degrade the quality of well-log correlation. And as a result; the surface seismic amplitude cannot be modeled reasonably well.

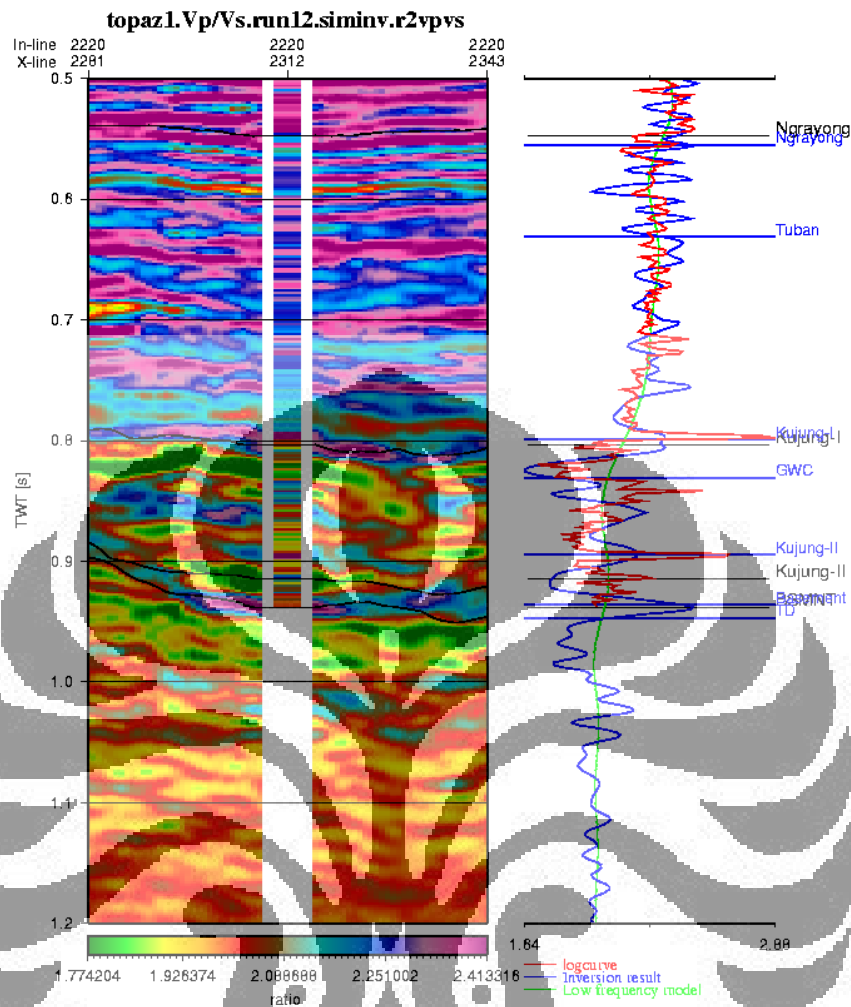


Figure 4.8. *Vp/Vs ratio inversion result and its comparison with measured Vp/Vs*

Last elastic attribute that was extracted in the exercise is the density. Density comes as the third term in Aki-Richards reflectivity modeling, which is the most non-linear parameter. Successful density inversion was required larger angle of angle stack, probably more than 45 degrees. However, as the target zone was quite shallow, 1.0 s, the surface seismic acquisition was not designed to be at larger angle. In the result, the expectation on good density result was not high. But we've seen in figure 4.9, within the target zone, we can see the density inversion result shows the same trend with measured density log responses.

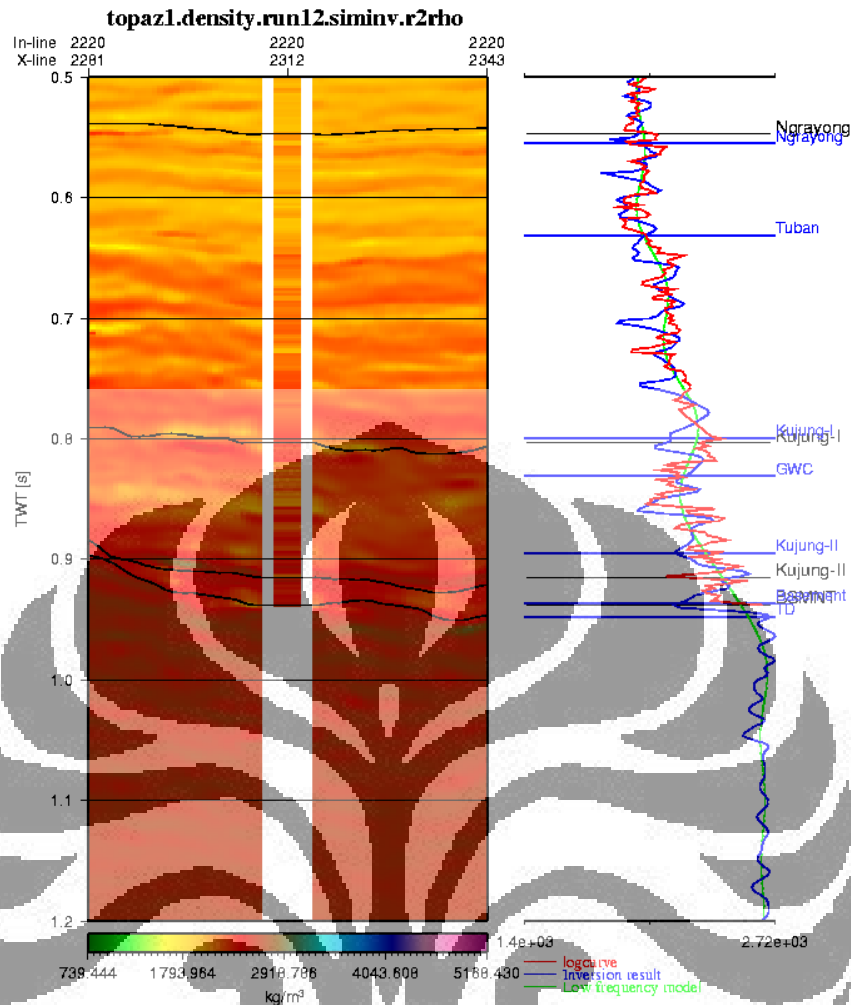


Figure 4.9. Density inversion result compared to measured density

It may conclude that inversion result was working as expected, considering the data quality and amount of well log information that are available. Analysis on the lateral map was carried out; this was done by extracting time slice around 0.8 s approximately the top of reservoir. The Kujung carbonate was interpretable in the amplitude time slice, but without any reservoir properties information. The same extraction process applied to AI and Vp/Vs cube, the Kujung-I hydrocarbon potential was localized in the flank of Kujung carbonate. Acoustic impedance slice shows high impedance value, which makes sense for a carbonate. The drop in Vp/Vs ratio in the same zone was interpreted probably due to presence of gas. Furthermore, in next chapter about Bayesian lithology classification it will be shown the relation between AI and Vp/Vs ratio to cluster this gas pay zone, and mapped into 3D space along with the confidence level.

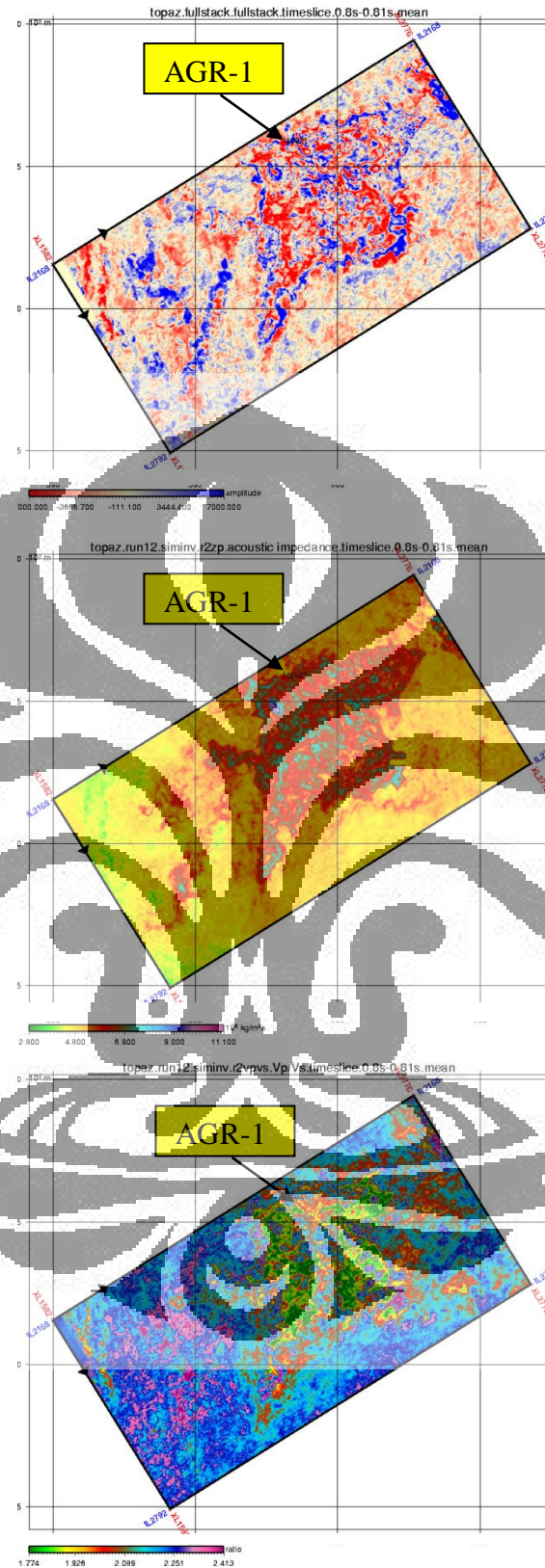


Figure 4.10. Comparison of time slice fullstack amplitude, AI cube, and Vp/Vs cube

CHAPTER 5

BAYESIAN RESERVOIR CHARACTERIZATION

Chapter V is the final analysis on Bayesian reservoir characterization. Analysis on well log scale has been carried out to get the understanding of how the characteristic of pay and non-pay zone. In chapter IV, workflow of how to derive elastic attribute in 3D space from seismic data via simultaneous seismic inversion has been explained. In this chapter analyses on Bayesian theorem to classify of fluid (wet or gas) from seismic inversion result is explained, and also analyses to extract porosity and saturation through Bayesian theorem and stochastic modeling.

5.1. Fluid Classification

Let us recall our discussion on Bayesian theorem. There are two things that were needed to run classification based on Bayesian theorem. One is the prior probability density function; the second is the likelihood function. In this study an equiprobable prior can be used for each fluid class (in this case noninformative means that each of the two fluid units has an equiprobable 50% chance of occurring at any point in the subsurface). The likelihood function will be derived based on rock physics template analysis from chapter 3.1 and the likelihood function was defined from elastic attributes as a result of seismic inversion.

Fluid classification is limited into two classes, they are gas and wet only. We now need to recall the rock physics template, where we can see the separation of gas and wet zone. We can set zone of these two classes, they are,

- Class I (Gas)
 - AI range : $3.9 \times 10^6 - 60. \times 10^6 \text{ Kg/m}^2\text{s}$
 - Vp/Vs range : 0 – 1.9
- Class II (Wet)
 - AI range : $4.0 \times 10^6 - 10.0 \times 10^6 \text{ Kg/m}^2\text{s}$
 - Vp/Vs range : 2.0 – ~

Other petrophysical parameters were used to define the zone such as V_{cl} and Sw . In this case using Sw less than 65% and total porosity above 10% as the cutoff of pay zone will do good separation. Probability density function (PDF) is derived from both class, as the representation of the variability in the formation properties. To match seismic frequency, the well logs are upscaled. Figure 5.1 showing contour of PDF for each class, green is wet class, and red is gas class. Two panel figures below it, showing PDF of each class for individual attribute, that is acoustic impedance and V_p/V_s ratio. In contour plot, data with the highest frequency occurrence will be marked with denser contour. When we project to specific axis (AI or V_p/V_s ratio) we can see the distribution of this value in terms of their frequency.

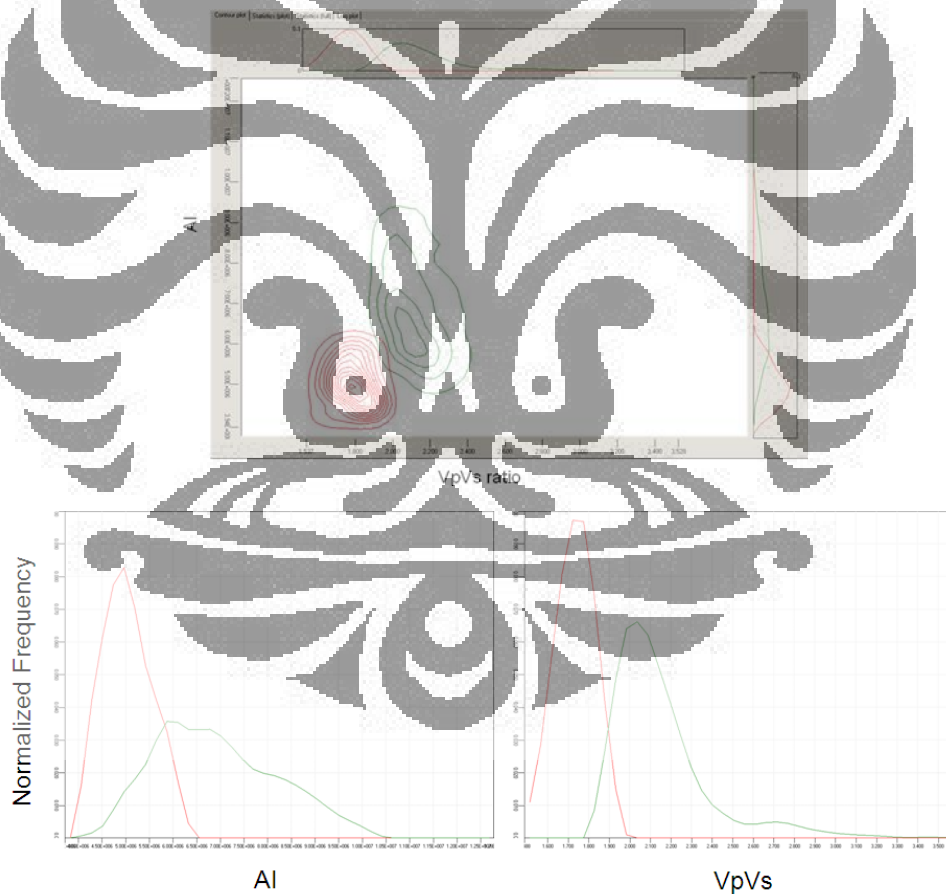


Figure 5.1. Prior Distribution

As prior PDF was built based on AI and Vp/Vs crossplot, it is only needed to integrate AI cube and Vp/Vs cube. The following figure (figure 5.2) shows the comparison of conventional seismic amplitude (right) with classification result (left) for inline that crossing AGR-1 well.

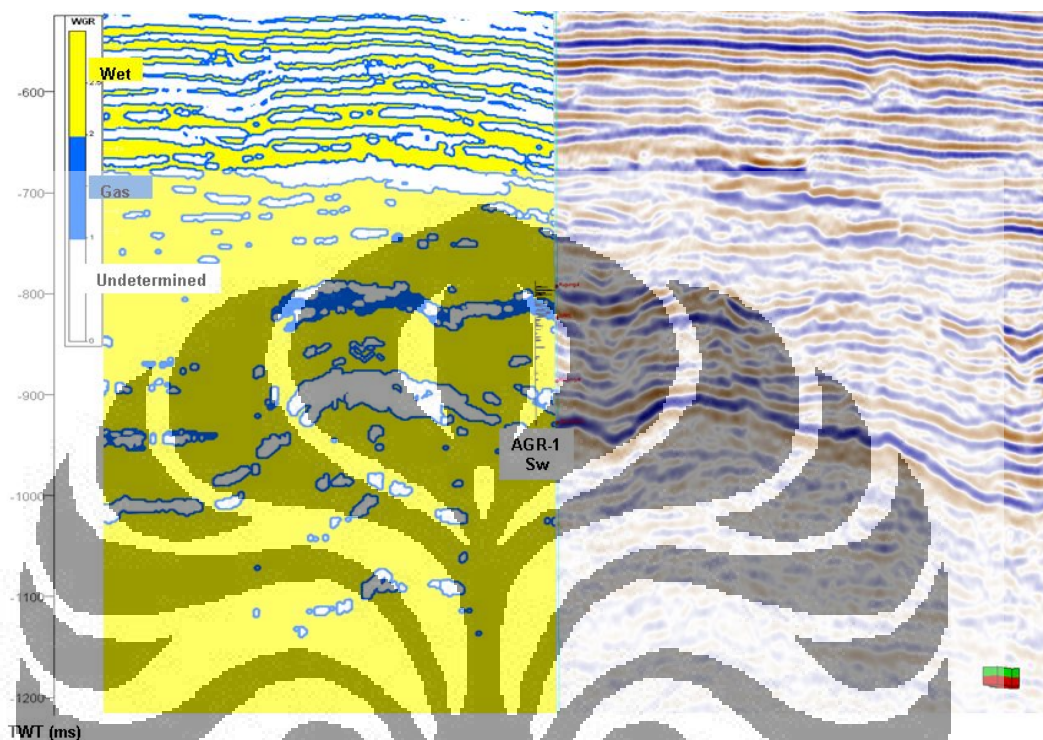


Figure 5.2. Comparison of fluid classification (left) with fullstack amplitude (right). Black curve in the middle is Sw.

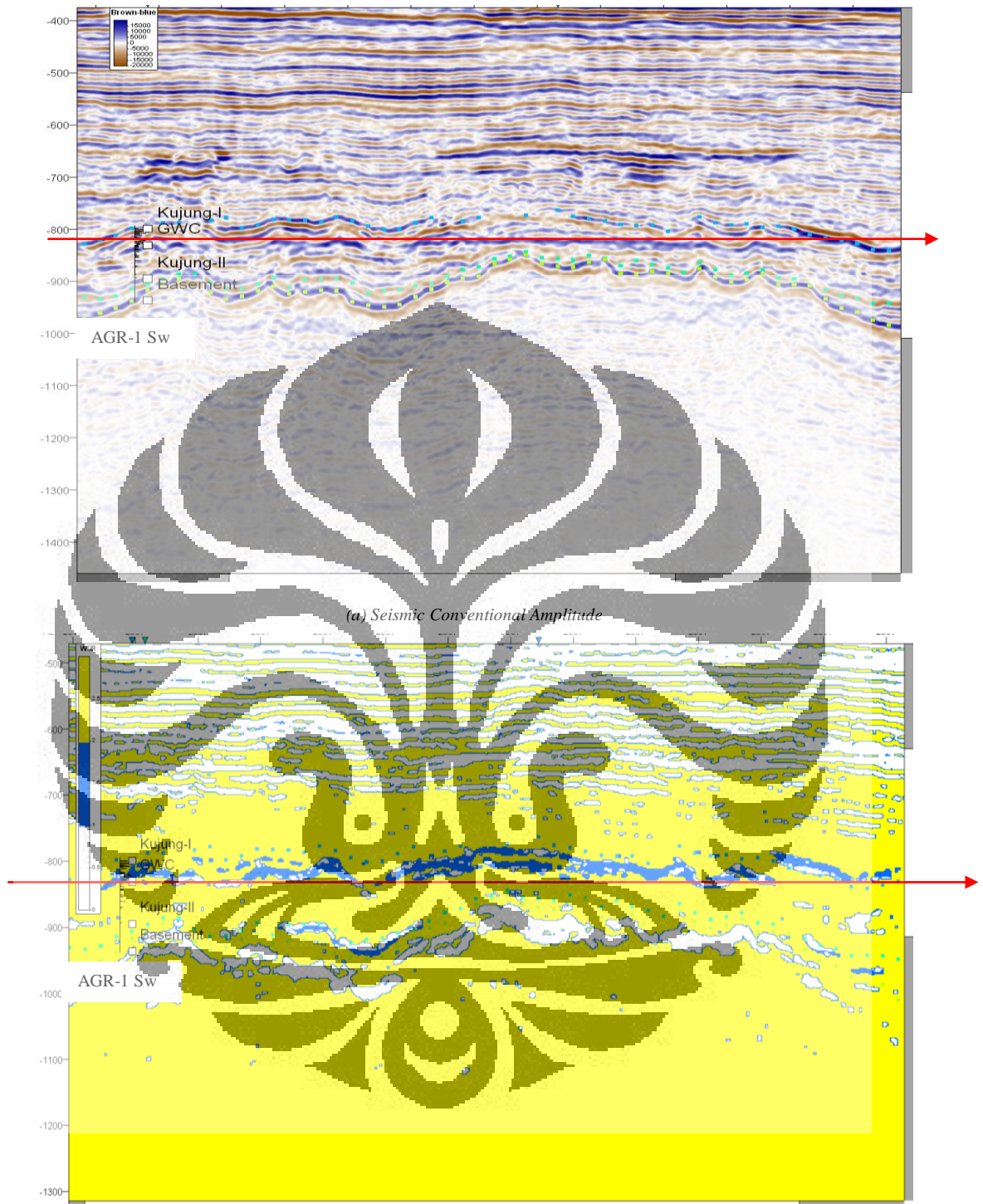
Blue in the figure 5.2 above is classified as gas, yellow is water, and white is undetermined class. The comparison between classification and Sw in the well, showing reasonable match, where we expected that our reservoir is slightly above GWC. We talked a little bit about flat spot anomaly in the data, after we did the classification, we are now can have confidence in saying that this is the GWC contact. Since only one well built the likelihood PDF, sometimes the classification will be biased towards the only one well. Even though, degree of confidence in classification is actually quite high, considering the separation of gas and wet is obvious in AI vs Vp/Vs ratio crossplot. This needs to be addressed further in the analysis.

The analysis from Kujung-I horizon slice on seismic amplitude data showed that seismic amplitude cannot clearly distinguish the reservoir zone. It is the inversion

that helps to increase the information content by transforming the boundary properties to layer properties. Other advantage of having seismic inversion as guide to map this attribute in 3D space is because spatial distribution is controlled by measured seismic amplitude. We reduce the bias effect due to limited well information.

Furthermore, quality control on inversion result observed how the inversion will shape the classification. Coming back again to figure 4.10, it is noticed that how V_p/V_s ratio drop is localized in within Kujung-I closure. By comparing this figure with following classification map (figure 5.4 and 5.5), classification is just another thing to convince and separate where the pay zone is. In figure 5.3.a. we see the flat spot that was observed clearly in the seismic amplitude marking the GWC, comparison with figure 5.3.b we defined the the zone above GWC as gas class. If we compare this classification with inversion result, AI inversion is shown in figure 5.3.e, and V_p/V_s Inversion is shown in figure 5.3.d, we observed how inversion will shape the classification result. The good thing about Bayesian classification is: it's not just classifying the pay zone, but also classify it with certain degree of confidence. The classification will be based on prior probability density function from well logs. In the 3D map figure 5.4 and 5.5, it is show the potential reservoir pay zone is distributed along carbonate build up flank.

Nevertheless, if the pay zone can be separated clearly in likelihood model definiton, Bayesian classification is a good tools to map the potential pay by integrating it with elastic attribute. But even though, when the pay zone can not be separated clearly, Bayesian theorem will give you how big is the probability of potential pay zone is.



(b) Classification Result

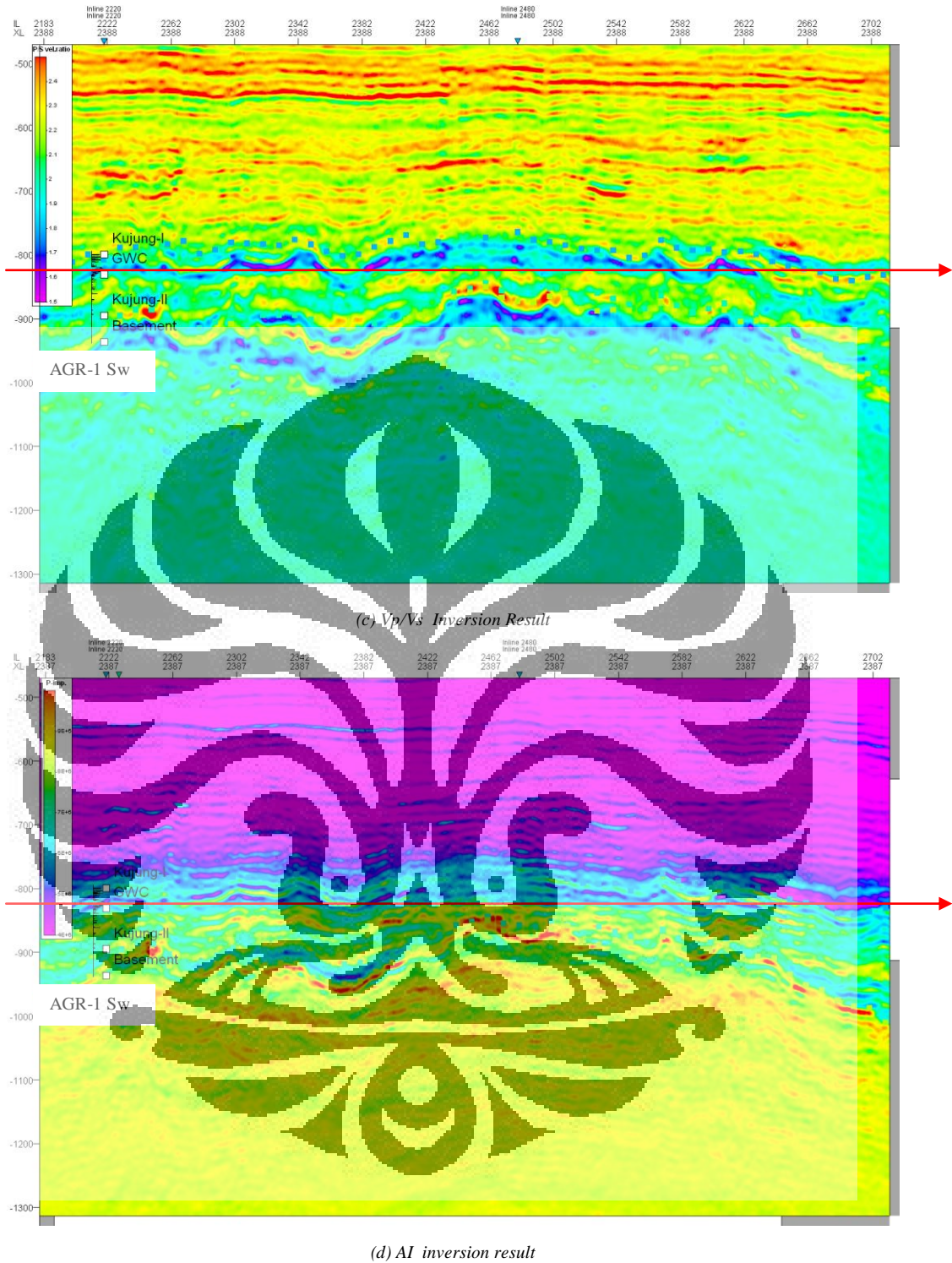


Figure 5.3. Comparison of seismic amplitude (a) with classification result (b), and the input for classification Vp/Vs (c) and AI (d) Noted that flat spot defined as boundary between gas and water, taken from offset XLine from AGR-1 well (log curve is Sw). Red arrow shows flatspot.

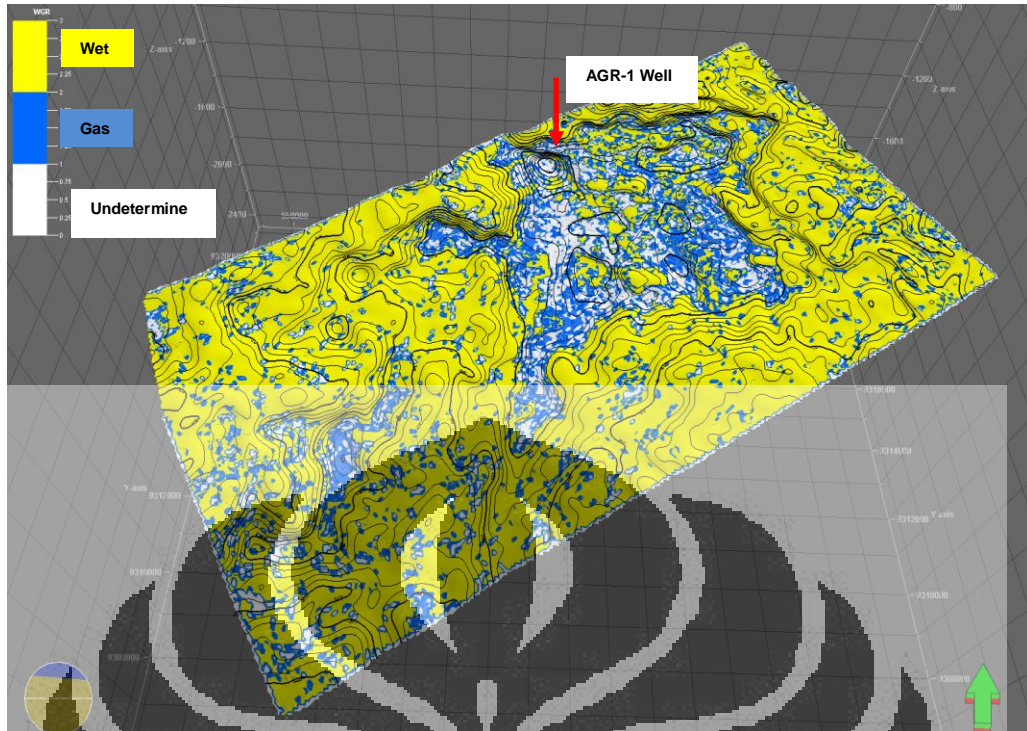


Figure 5.4. Time Structure with classification map as color scale from 25 ms below Kujung-I, blue is gas, yellow is wet, and white is undetermined

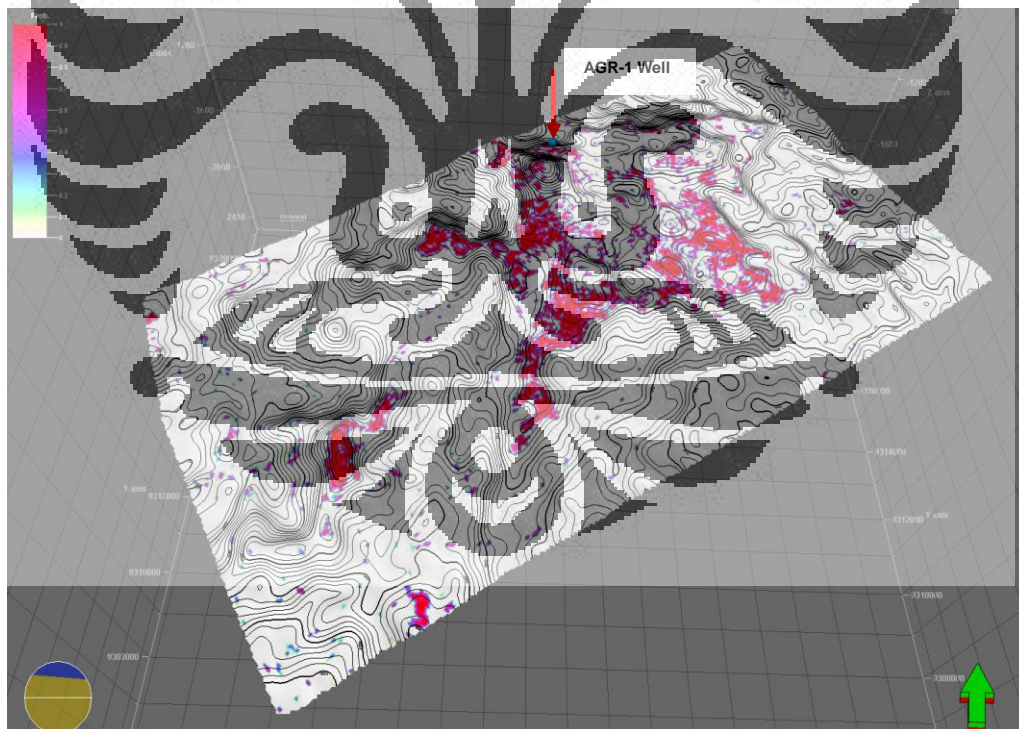


Figure 5.5. Time Structure map with gas probability as color scale from 25 ms below Kujung-I

5.2. Joint-Porosity Saturation Modeling

Having defined rock physics relationship between rock modulus and porosity, let us now see how to extrapolate this information into 3D space by doing stochastic modeling and Bayesian inversion. The modeling tries to generate large numbers porosity-saturation pairs with bulk modulus. By doing this, the simulation generated joint PDF between porosity and saturation to be used in Bayesian estimation. To remove high discrepancy between log scale and seismic scale, the log data was upscale to match the seismic frequency. Figure 5.6 (a) below shows the relationship between bulk modulus with porosity and shear modulus with porosity, the green line shows the Hashin-Shtrikman Upper Bound and Lower bound, meanwhile the orange line shows the non linear relationship between porosity with bulk modulus. The stochastic simulation will simulate bulk modulus response at specific porosity value given by this orange line. The blue line is the maximum allowed deviation from the orange line. Figure 5.6 (b) shows the crossplot between porosity and saturation.

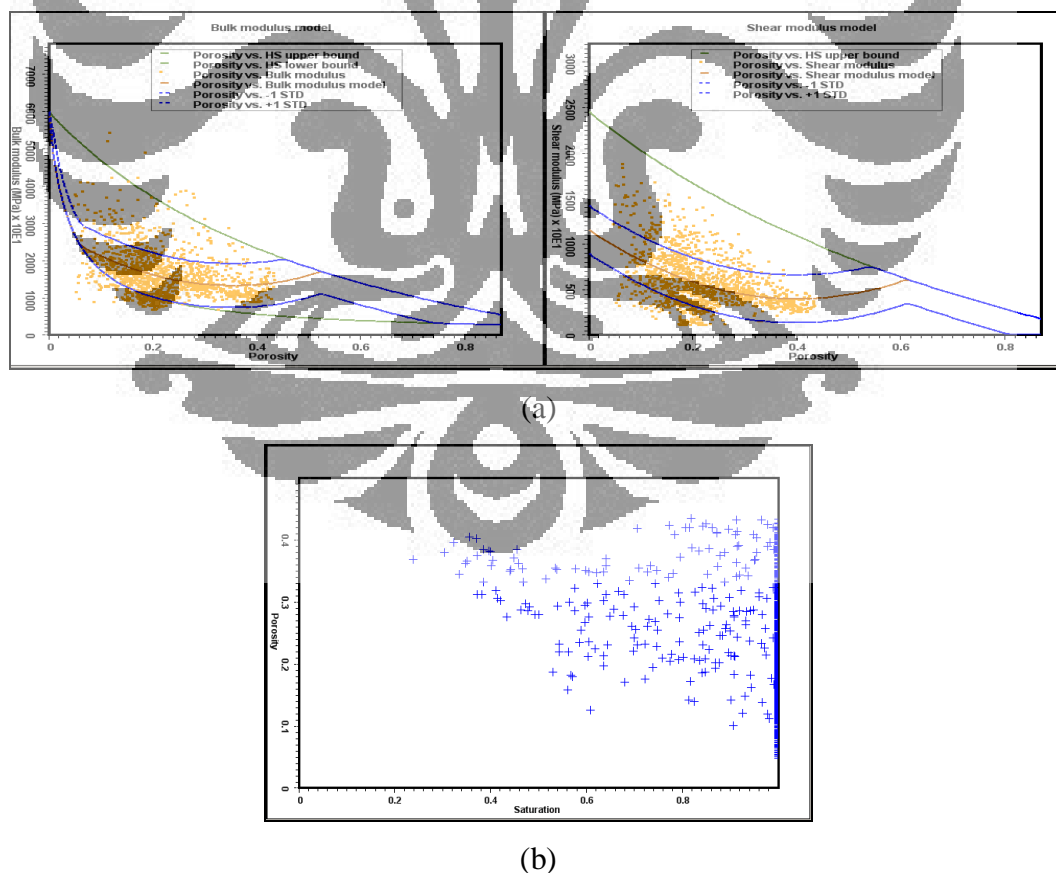


Figure 5.6. (a) Porosity-bulk modulus crossplot and 2nd order polynomial fitting, (b) Water saturation vs Porosity crossplot

The modeling will be bounded by Hashin-Shtrikman bound so that the modeling has more physical meaning. One million simulations were performed to generate large number of bulk and shear moduli also density from the random porosity-saturation realizations. The simulation limited to 8-40% porosity with 0-65% water saturation. Figure 5.7 below on left panel shows the simulation result. It is expected that simulation cover all data distribution. Right panel shows one of the joint PDF for AI: $7.5e6$ (kg/m².s), SI: $4.2e6$ (kg/m².s), RHO: 2100 kg/m³ elastic attribute parameters. This is basically said, the maximum probable value for saturation and porosity for given AI, SI, and RHO value as above, is 25% porosity with 65 % water saturation.

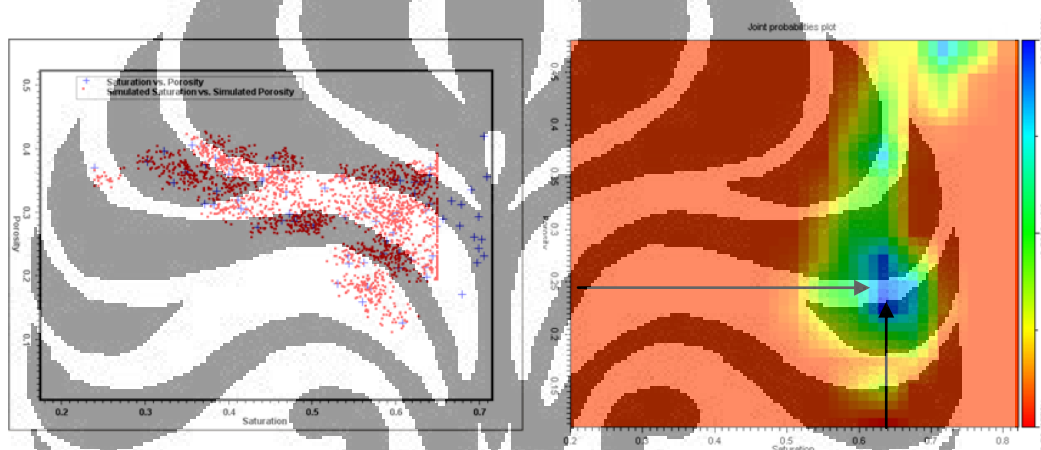
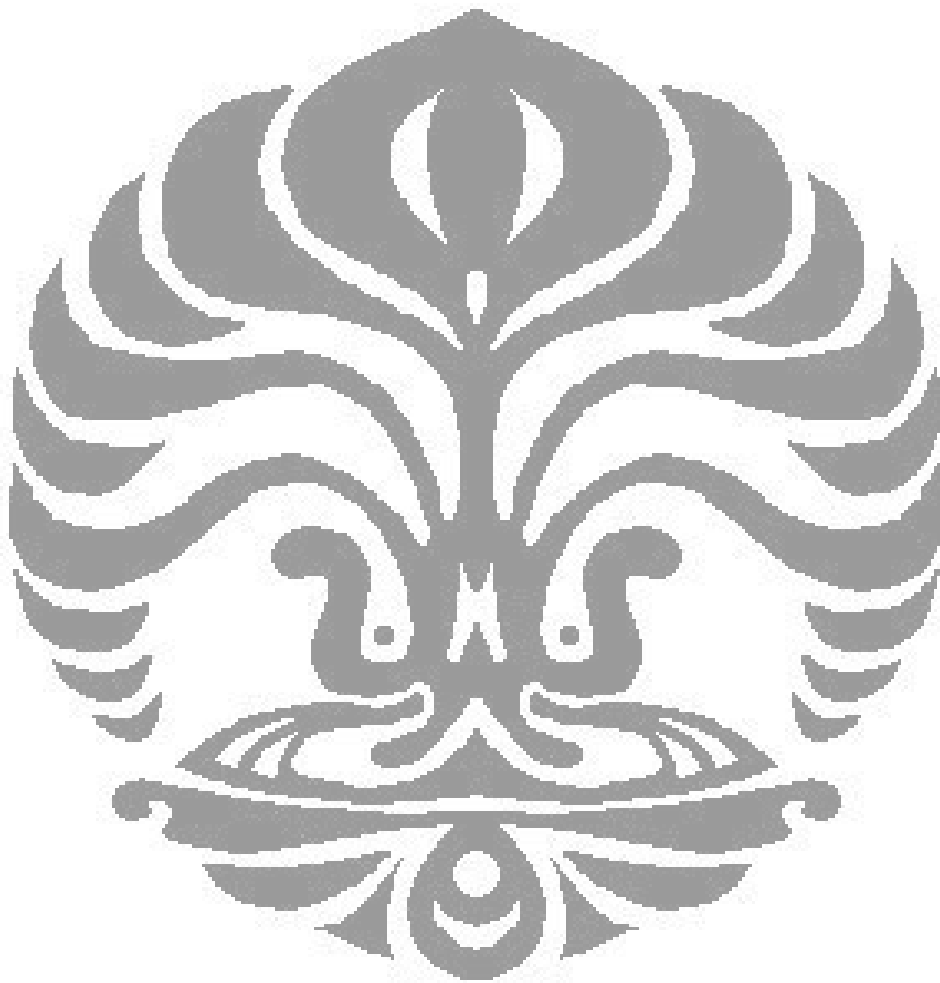


Figure 5.7. Simulation result (left) Joint porosity-saturation PDF (right)

To extrapolate this into 3D space, acoustic impedance, shear impedance, and density from simultaneous inversion will be used as the input for the inversion. These attributes will act as likelihood function for this Bayesian porosity-saturation estimation. This estimation is an extensive process, the estimation limited to only 80% pay zone confidence that was derived from previously fluid classification in order to reduce the workload.

Extracted porosity and saturation over zone of interest tend to be more uniform, this may due to mode of saturation and porosity is centralized on 60% water saturation came from one well only. Distribution of porosity over Kujung-I carbonate range from 15-25% porosity. Meanwhile the saturation ranged from 40%-60%. Final porosity value is the maximum a posterior from Bayesian

posterior PDF. With all the associated error in the porosity-bulk modulus modeling, what has been extracted from stochastic modeling is quite reasonable. Further research on careful mineralogy analysis may lead to more sophisticated modeling result. Analysis on 3D map (figure 5.9 and 5.10), characterize the potential pay zone with their approximate porosity and saturation.



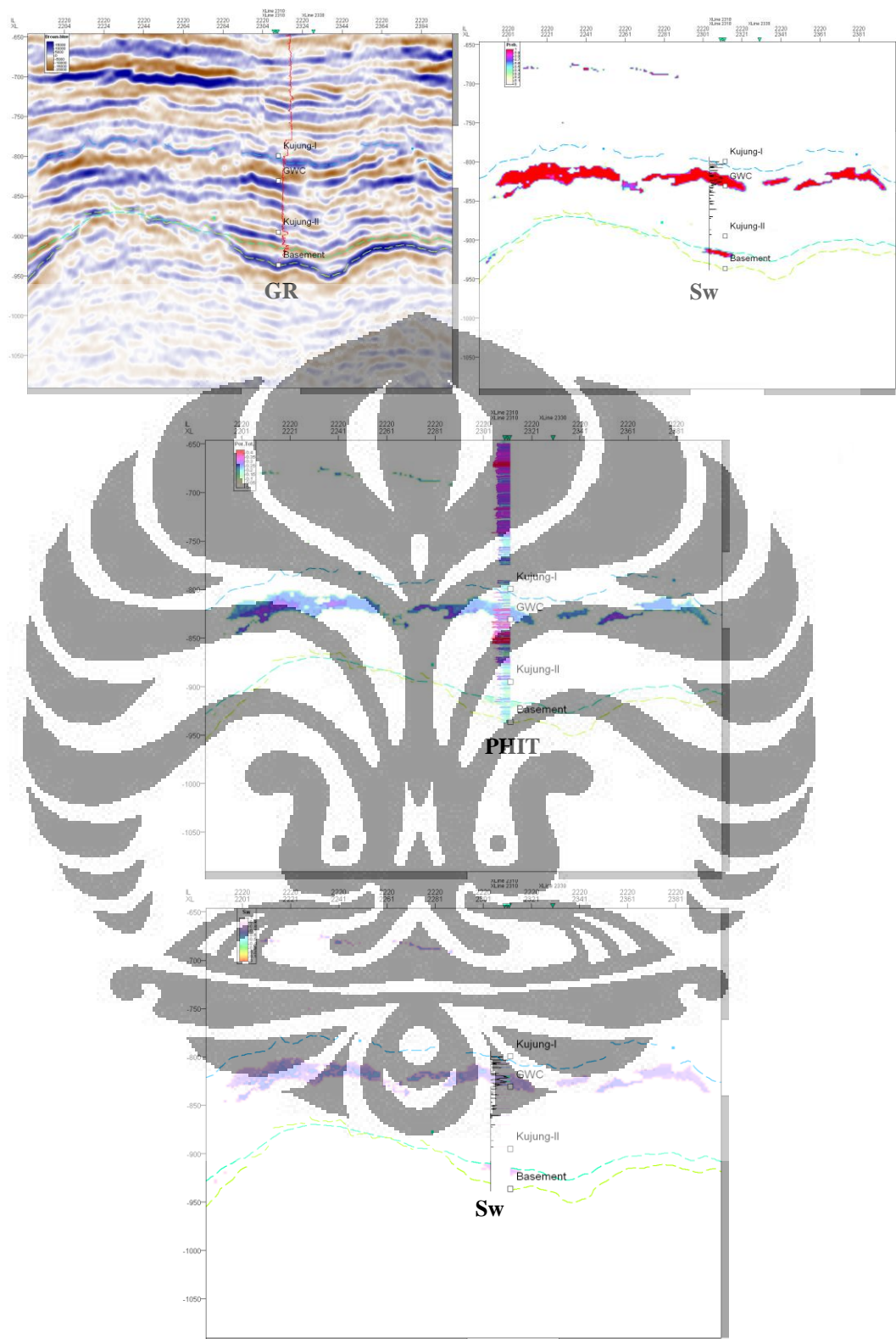


Figure 5.8. Comparison of seismic amplitude (top left), gas probability (top right), porosity (mid), and water saturation (bottom). AGR-1 well marked with inserted curve in the plot.

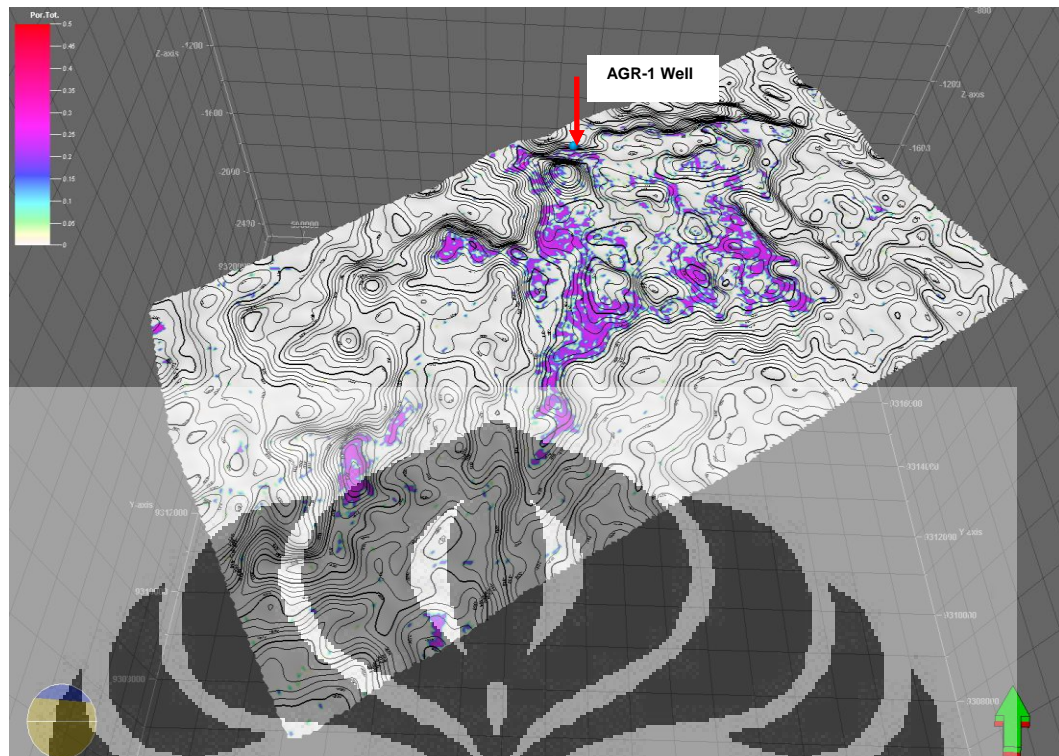


Figure 5.9. Time Structure map with porosity as color scale from 25 ms below Kujung-I

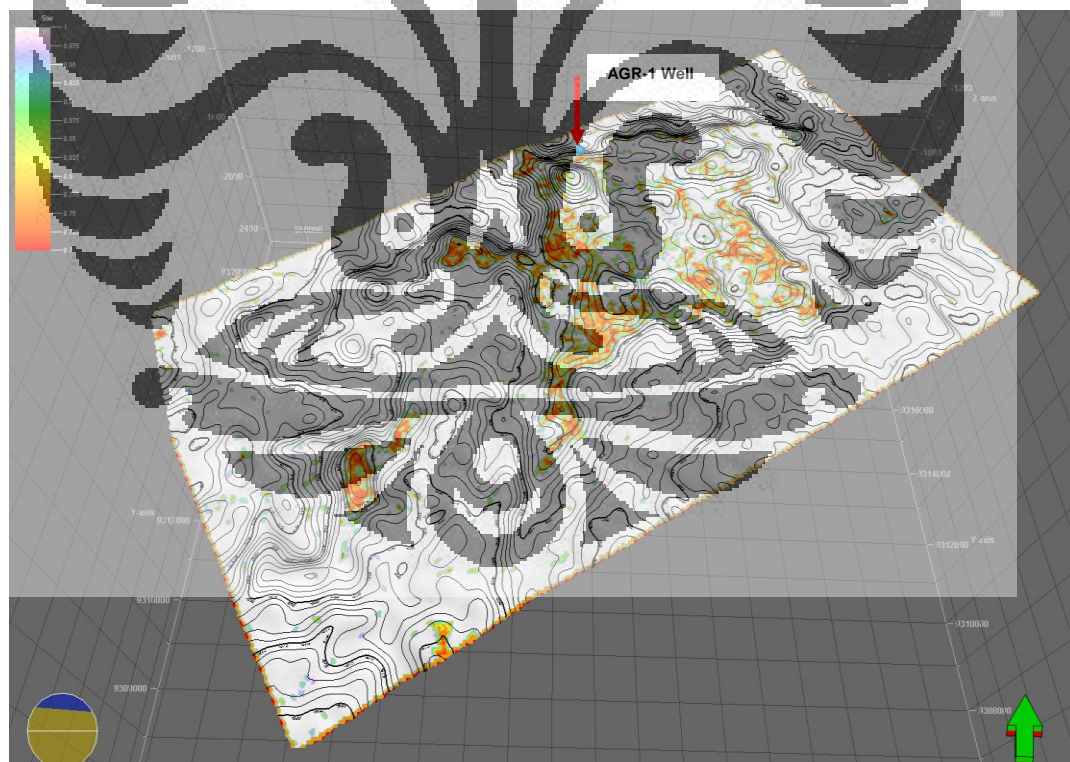


Figure 5.10. Time structure map with water saturation as color scale from 25 ms below Kujung-I

CHAPTER 6

DISCUSSION AND RECOMMENDATION

This study has presented a Bayesian reservoir characterization on a carbonate reservoir. The characterization include qualification of pay zone, this was done by doing fluid classification. I also presented quantification of each pay zone in terms of its porosity and saturation. The result is confirming the geological interpretation for this particular area.

The potential gas zone was lying slightly above GWC. Since GWC can be identified by flat spot, mapping this particular event will help to localize the gas. By analyzing the gas probability map, a conclusion can be drawn that the probable gas was localized in the structural high in the flank of the carbonate.

There are two things that I would like to discuss in the final chapter of this thesis,

Rock Physics Model for Carbonate

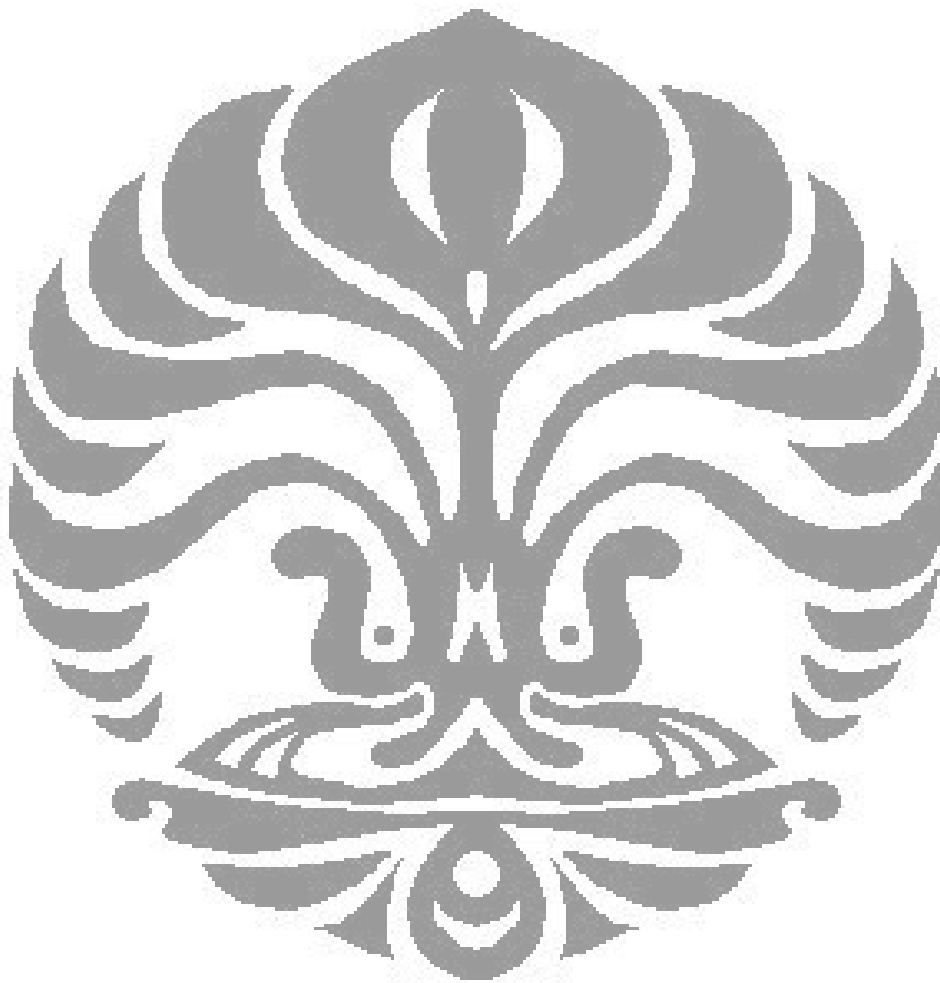
Fluid modeling in this study is oversimplified using Biot-Gassmann modeling. So far, the flaw that was seen in Biot-Gassmann theory for this case is when we use it for porosity and fluid saturation estimation. In fluid zoning estimation, Biot-Gassmann approach is still valid in area of study within reasonable error. For further research, I would suggest to use valid rock physics model in carbonate for all the analysis. Recent publication shows much improvement when doing carbonate rock physics analysis using effective medium theory. Once this model has been validated in the well, the inversion capability can be used to extrapolate this value to 3D space.

Porosity-Saturation Estimation

I have shown that Bayes theorem will be helpful in interpretation and judgment by associating the probabilities with certain degree of accuracy. Thus, using Bayesian inversion to extract non linear rock physics attribute such as porosity and

saturation will help the interpretation. Valid rock physics model also should be taken into account when dealing with this theorem.

In this thesis, I didn't discuss much about convergence and further justification in Bayesian theorem and estimation. I would suggest further and deeper research on Bayesian inversion to estimate rock physics parameter from seismic data.



REFERENCES

- Aki, K., and Richards, P.G., 1980, Quantitative Seismology: Theory and Methods, W.H. Freeman and Co., San Francisco, 932 pp
- Adam, L., Batzle, M. and Brevik, I., 2006, Gassmann's Fluid Substitution and Shear Modulus Variability in Carbonates at Laboratory Seismic and Ultrasonic Frequencies, *Geophysics*, 71, F173-F183
- Adriansyah and McMechan, G., 2001, AVA Analysis and Interpretation of a Carbonate Reservoir: Northwest Java Basin, Indonesia
- Carter, D., C., Mandhiri, D., Park, R.K., Asjhari, I., Basyuni, S., Birdus, S., Bradfield, J.P., Iriawan, A., Nasfiah, M., and Nugroho, M.A.A., 2005, Interpretation Methods in The Exploration of Oligocene-Miocene Carbonate Reservoirs, Offshore Northwest Madura, Indonesia, Indonesian Petroleum Association Proceeding, August 2005
- Baechle, G.T., 2005, Changes of Shear Moduli Carbonate Rocks: Implications for Gassmann Applicability, *The Leading Edge*, May 2005, 507-510
- Bachrach, R., Beller, M., Liu, C. C., Perdomo, J., Shelander, D., and Dutta, N., 2004, Combining Rock Physics Analysis, Full Waveform Prestack Inversion and High-Resolution Seismic Interpretation to Map Lithology Units in Deep Water: A Gulf of Mexico Case Study, *The Leading Edge*, 2004, 378-383
- Bhachrach R., 2006, Joint Estimation of Porosity-Saturation Using Stochastic Rock-Physics Modeling, *Geophysics* 71, 53-63
- Biot, M.A., 1956, Theory of Propagation of Elastic Wave in a Fluid Saturated Porous Solid, *J. Acoust. Soc. Am.* 28, 168-191
- Chacko, S., 1989, Porosity Identification Using Amplitude Variations with Offset: Examples from South Sumatra, *Geophysics*, 54, 942-951
- Connolly, P. 1999, Elastic Impedance, *The Leading Edge* 18, April 438-542
- Gassmann, F., 1951, *Über die Elastizität poröser Medien*. *Vier. der Natur. Gesellschaft in Zurich*, 96, 1-23
- Grandis, H., Menvielle, M. and Roussinol, M., Thin-sheet electromagnetic

- inversion modeling using Monte Carlo Markov Chain (MCMC) algorithm, *Earth Planets Space*, 54, 511–521,
- Ma, X-Q, 2002, Simultaneous Inversion of Pre-Stack Seismic Data for Rock Properties Using Simulated Annealing, *Geophysics*, 67, 1877-1885
- Maver K.G. and Rasmussen, K.B., 2004, Simultaneous AVO Inversion for Accurate Prediction of Rock Properties, *Offshore Technology Conference*, May 2004
- Mavko G., Mukerji and T., Dvorkin, J., 1998, *Rock Physics Handbook*, Cambridge University Press
- Munadi, S., 2000, *Aspek Fisis Seismologi Eksplorasi*, Catatan Kuliah, Universitas Indonesia
- Munadi, S., 2005, *Pengantar Geostatistik*, Catatan Kuliah, Universitas Indonesia
- Murdianto, B., 2007, *Bayesian Approach for Constraining Facies Simulations with Seismic Information*, Master Thesis, Dept. Of Physics, University of Indonesia
- Pearl Energy Internal Report, 2009,-
- Rasolofosaon, P., Lucet, N., and Zinszner, B., 2008, Petroacoustic of Carbonate Reservoir Rocks, *The Leading Edge* 27, August 2008
- Santosa, B., 2007, *Data Mining: Teori dan Aplikasi*, Graha Ilmu